Neutrino-nucleus reaction cross sections and e-capture rates based on recent advances in shell-model interactions

Toshio Suzuki
Nihon University,
NAOJ, Tokyo

INT, Seattle

March 9, 2018

- New shell-model Hamiltonians obtained due to the advances of studies of exotic nuclei and describe well the spin modes in nuclei

SFO (p-shell: p-sd); CK-MK-KB+monopole correction: GT in ^{12}C, ^{14}C

Suzuki, Fujimoto, Otsuka, PR C69 (2003)

USDB (sd-shell); Brown , Richter, PR C74 (2006)

SDPF-M (sd-shell:sd-$f_{7/2}p_{3/2}$); USD+mon. cor.: Utsuno et al, PR C60 (1999)

GXPF1J (fp-shell): GT in Fe and Ni isotopes, M1 strengths

Honma, Otsuka, Mizusaki, Brown, PR C65 (2002); C69 (2004)

VMU (monopole-based universal interaction)

Otsuka, Suzuki, Honma, Utsuno et al., PRL 104 (2010) 012501

Systematic improvements in energies, magnetic moments, GT strengths

* important roles of tensor force

Monopole terms of V_{NN}

$$V_M^T(j_1j_2) = \frac{\sum_J (2J+1) < j_1j_2;JT \,|\, V \,|\, j_1j_2;JT >}{\sum_J (2J+1)}$$

Monopole terms of V_{NN}

$j_>(=\ell+1/2) - j_<(=\ell-1/2)$: attractive

$j_> - j_>,\ \ j_< - j_<$: repulsive

Otsuka, Suzuki, Fujimoto, Grawe, Akaishi, PRL 69 (2005)

tensor force

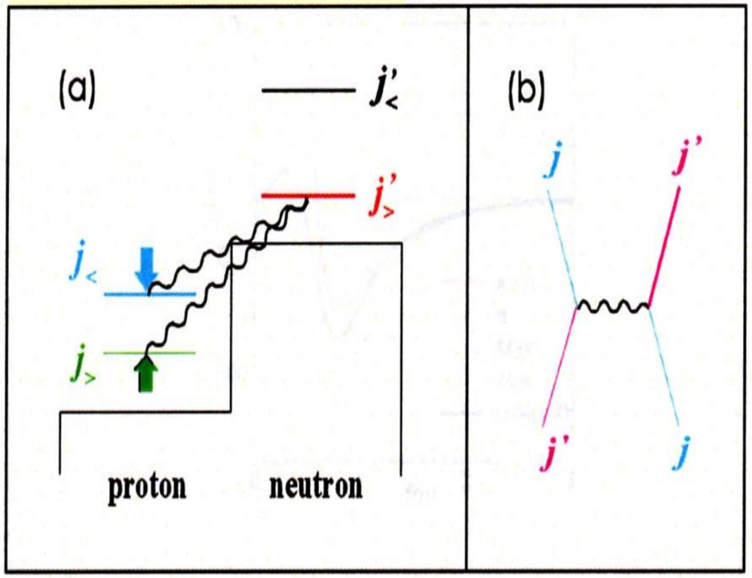

Tensor forces due to π+ρ meson exchanges

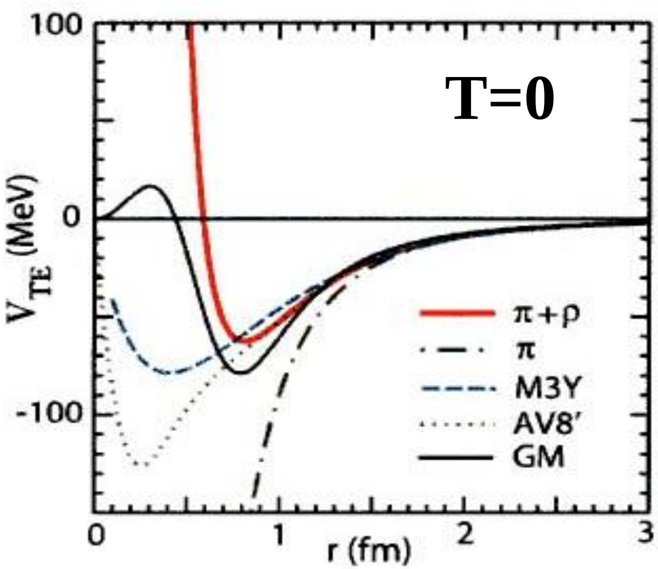

$$V_T = \frac{1}{3}\vec{\tau}_1 \cdot \vec{\tau}_2 S_{12}\{\frac{f^2}{4\pi} Y_2(m_\pi r) - \frac{f_\rho^2}{4\pi} Y_2(m_\rho r)\}$$

$$S_{12} = 3\vec{\sigma}_1 \cdot \hat{r}\vec{\sigma}_2 \cdot \hat{r} - \vec{\sigma}_1 \cdot \vec{\sigma}_2 \qquad Y_2(x) = (1 + \frac{3}{x} + \frac{3}{x^2})\frac{e^{-x}}{x}$$

$$\frac{f^2}{4\pi} = 0.08, \qquad \frac{f_\rho^2}{4\pi} = 4.86 \ \ (\frac{f_\rho^2}{m_\rho^2} = 2\frac{f_\pi^2}{m_\pi^2})$$

Tensor component: renormalized ≈ bare

tensor = π+ρ meson exchange with short- range correlation

VMU: monopole-based universal interaction

Otsuka, Suzuki, Honma, Utsuno, Tsunoda, Tsukiyama, Hjorth-Jensen, RL 104 (2010) 012501

Monopole terms: New SM interactions vs. microscopic G matrix

tensor force → characteristic orbit dependence: kink

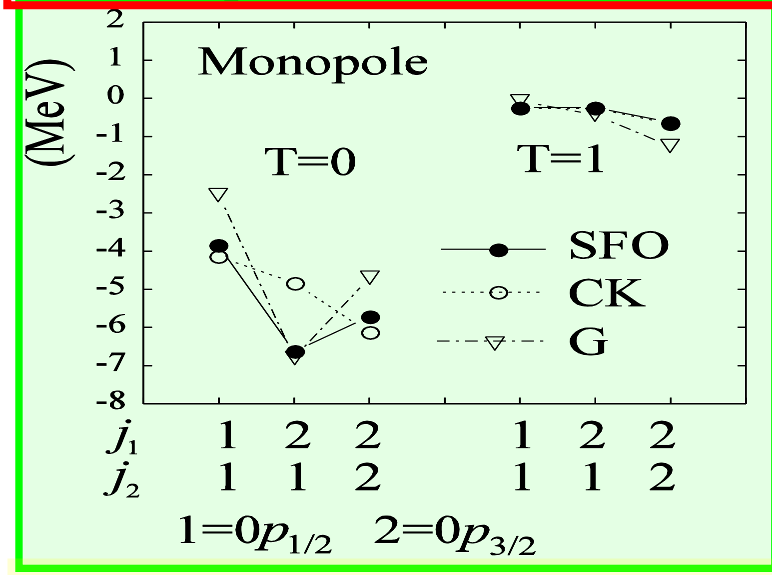

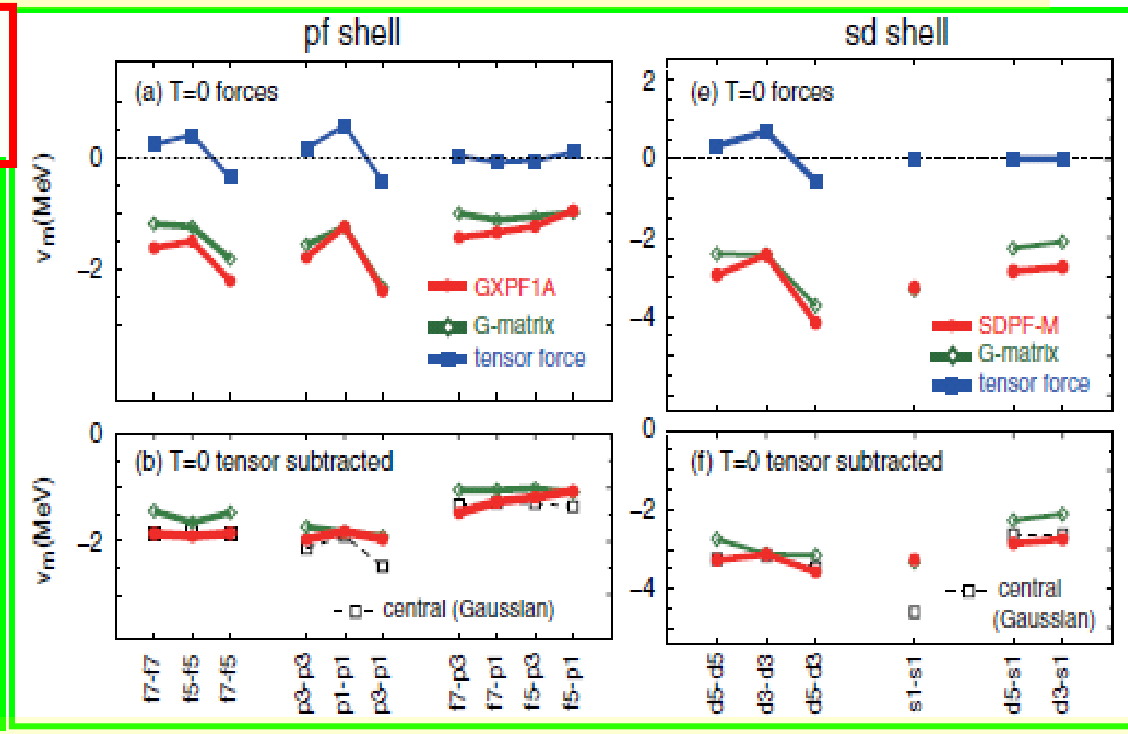

Proper shell evolutions toward drip-lines: Change of magic numbers

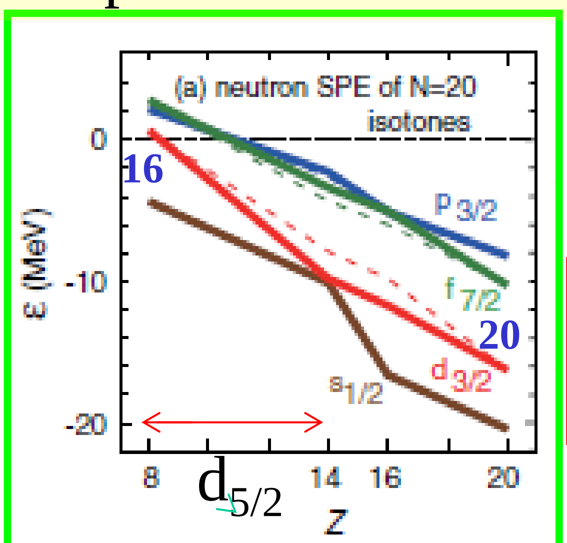

Effective single-particle energy:

$$E_{eff}(\nu j) = \varepsilon(\nu j) + \sum_{j'} n(\nu j') V_M^{T=1}(j,j') + \sum_{j'} n(\pi j') V_M^{np}(j,j')$$

$\pi d_{5/2} - \nu d_{3/2}$ attraction

$\varepsilon(\nu j)$ = s.p.e for the core

e.g. N=20 isotones

core = ^{16}O

[dashed box] =s.p.e for ^{28}O

ν-nucleus reactions: $E_\nu \leq 100$ MeV

ν-^{12}C, ν- ^{13}C, ν-^{16}O, ν-^{56}Fe, ν-^{56}Ni, ν- ^{40}Ar

- low-energy ν-detection
  Scintillator (CH, …), H_2O, Liquid-Ar, Fe
- nucleosynthesis of light elements in supernova explosion
- ν-oscillation effects

e-capture rates in stellar environments

- sd-shell: cooling of O-Ne-Mg core in stars by nuclear URCA processes
  USDB vs ab initio interactions (chiral effective int.)
- pf-shell: Type-Ia SNe and nucleosynthesis of iron-group elements
- sd-pf shell nuclei in the island of inversion
  EKK (extended Kuo-Krenciglowa method)

▪ν-nucleus reactions

p-shell: SFO

pf-shell: GXPF1J (Honma et al.)

cf. KB3 Caurier et al.

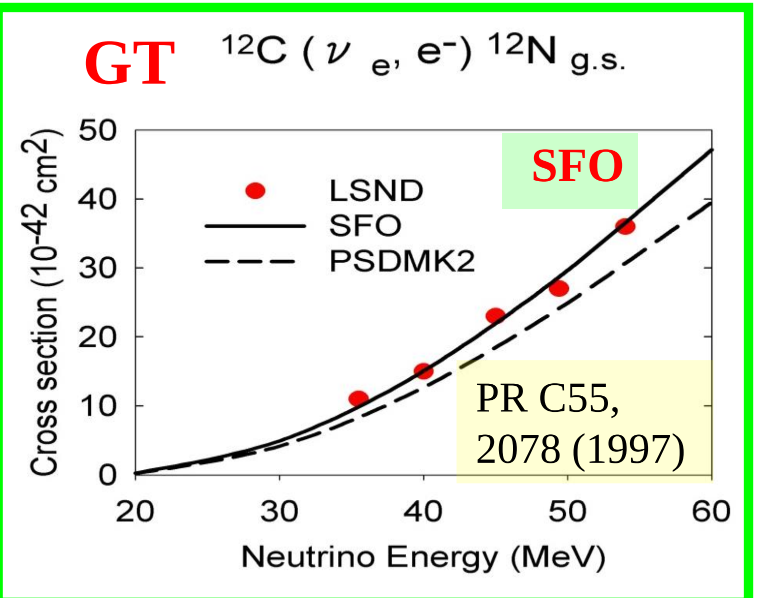

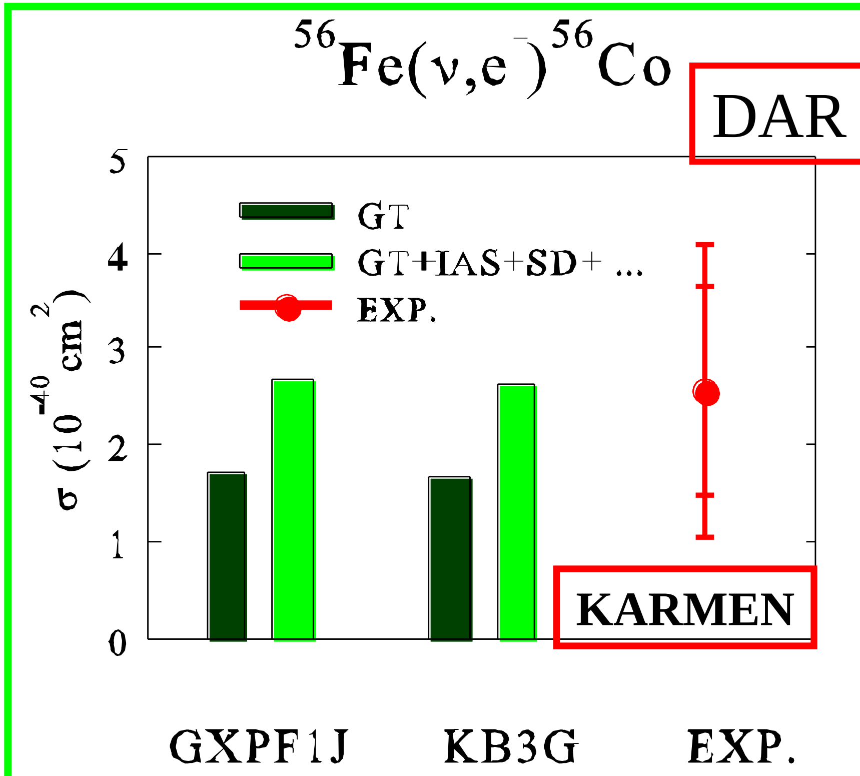

Suzuki, Chiba, Yoshida, Kajino, Otsuka, PR C74, 034307, (2006).

SFO: g_A^{eff}/g_A=0.95
B(GT: 12C)_cal = experiment

B(GT)=9.5 $B(GT)_{exp}$=9.9±2.4 $B(GT)_{KB3G}$=9.0

SD + … : RPA (SGII)

(ν, ν'), (ν_e, e^-) SD exc.
SFO reproduces DAR cross sections

$$\langle\sigma\rangle_{exp} = (256 \pm 108 \pm 43) \times 10^{-42}\ \mathrm{cm}^2.$$
$$\langle\sigma\rangle_{th} = (258 \pm 57) \times 10^{-42}\ \mathrm{cm}^2.$$

SM(GXPF1J)+RPA(SGII) 259 x10^{-42}cm^2
RHB+RQRPA(DD-ME2) 263
RPA(Landau-Migdal force) 240

^{12}C

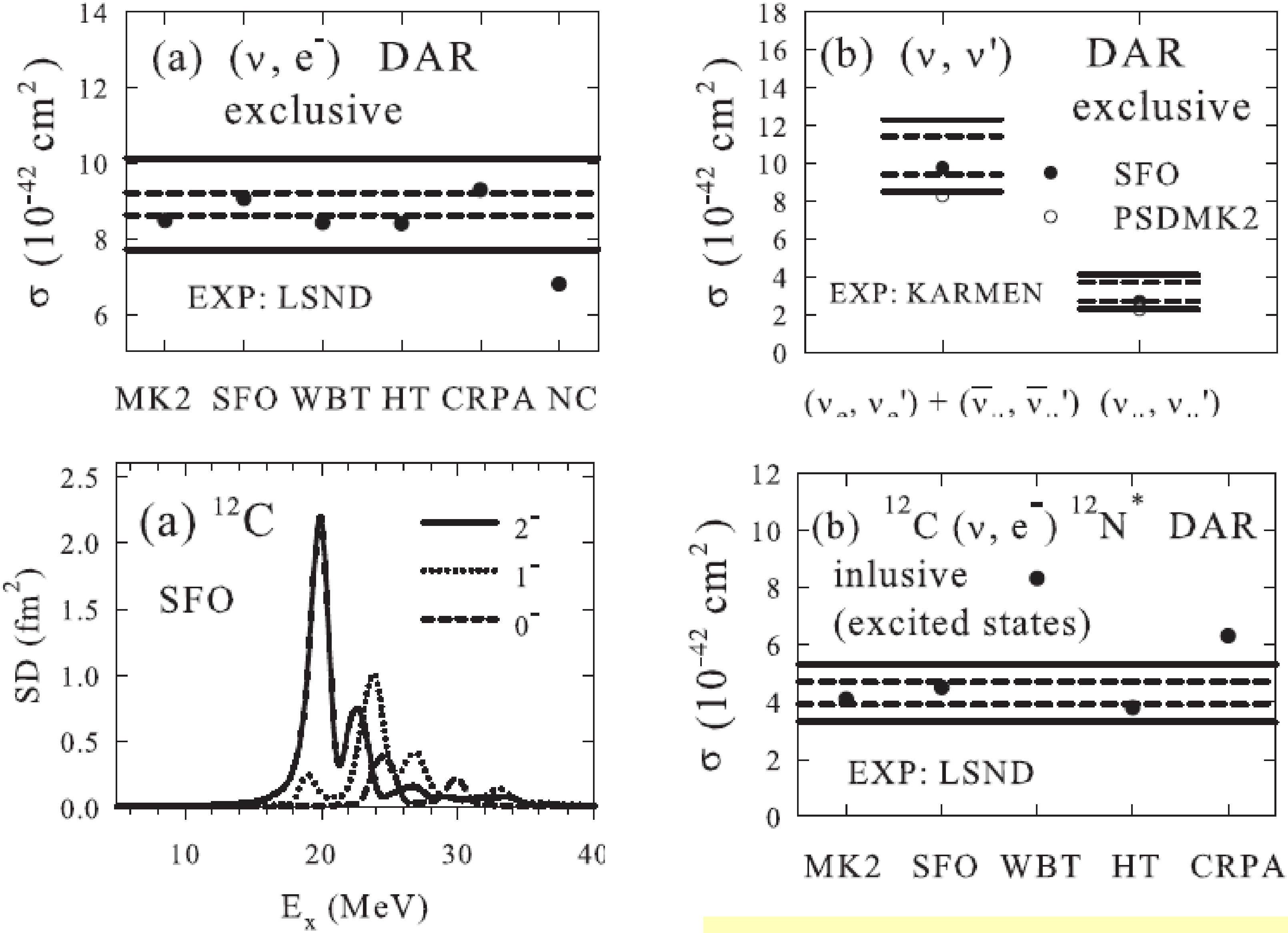

HT: Hayes-Towner, PR C62, 015501 (2000)
CRPA: Kolb-Langanke-Vogel, NP A652, 91 (1999)

^{12}C Neutral current reactions ^{12}C

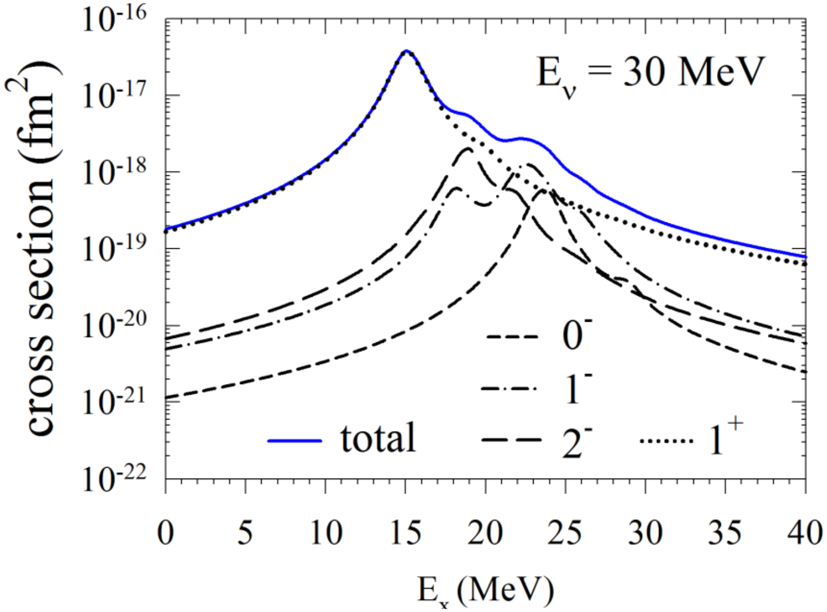

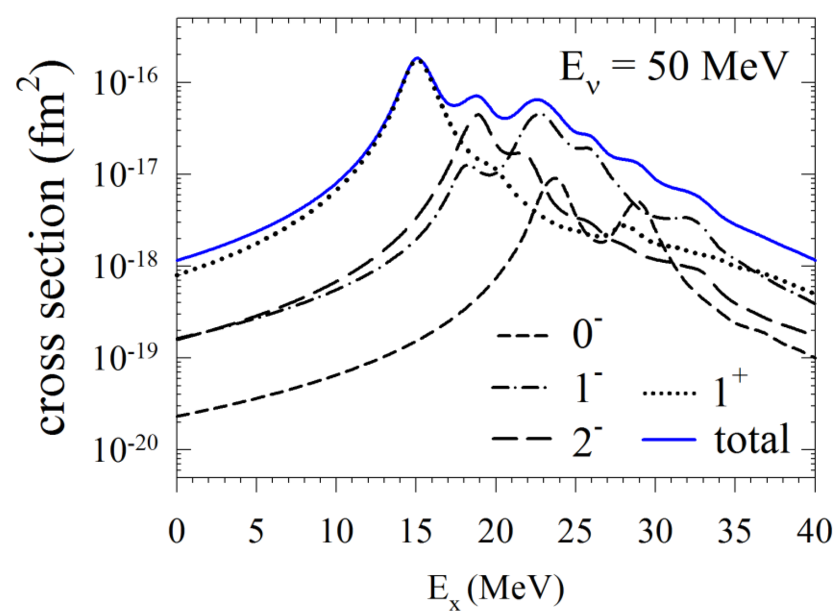

^{12}C 1^+

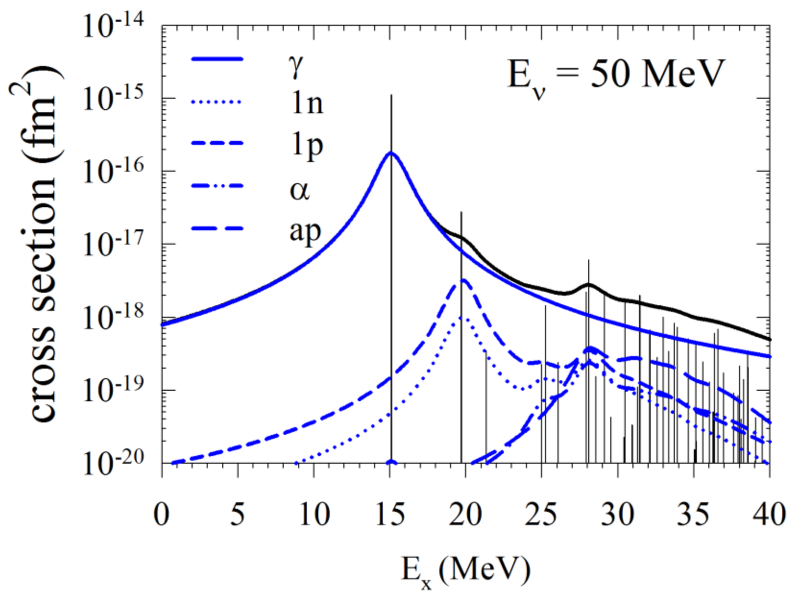

^{12}C 2^-

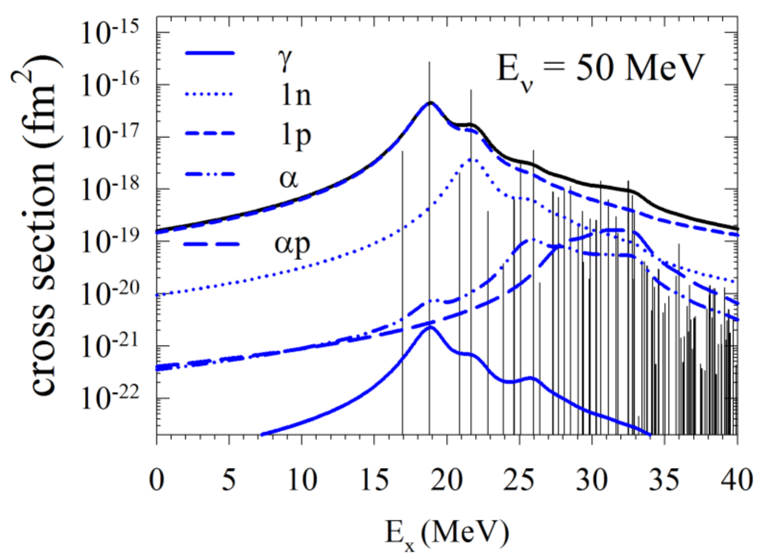

▪Nucleosynthesis processes of light elements in SNe

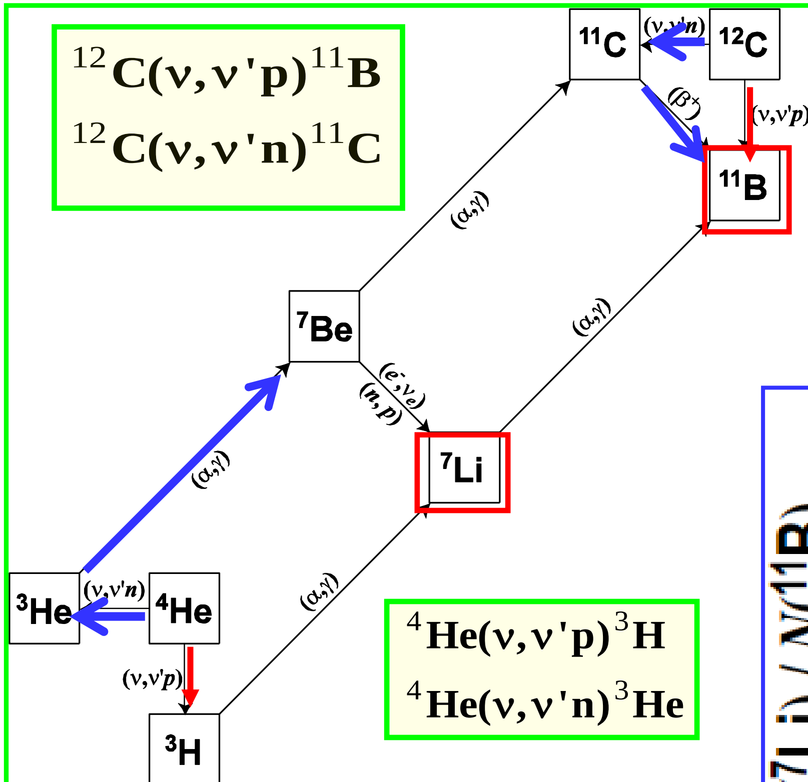

Enhancement of ^{11}B and ^{7}Li abund

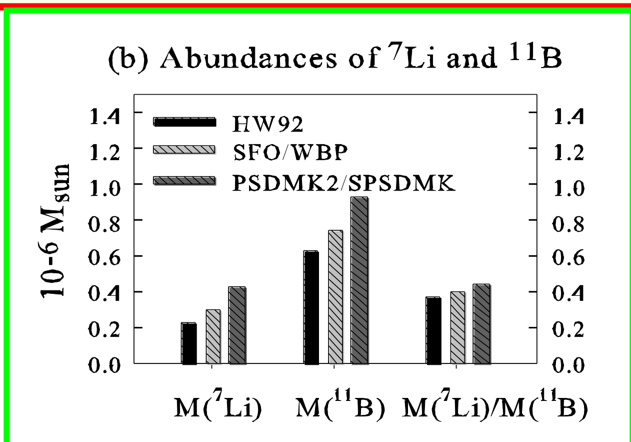

Effects of MSW ν oscillations

$$\text{Normal}-\text{hierarchy}: \nu_\mu, \nu_\tau \rightarrow \nu_e$$

Increase in the rates in the He layer:

4He(ν_e,e^-p)3He **12C(ν_e,e^-p)11C**

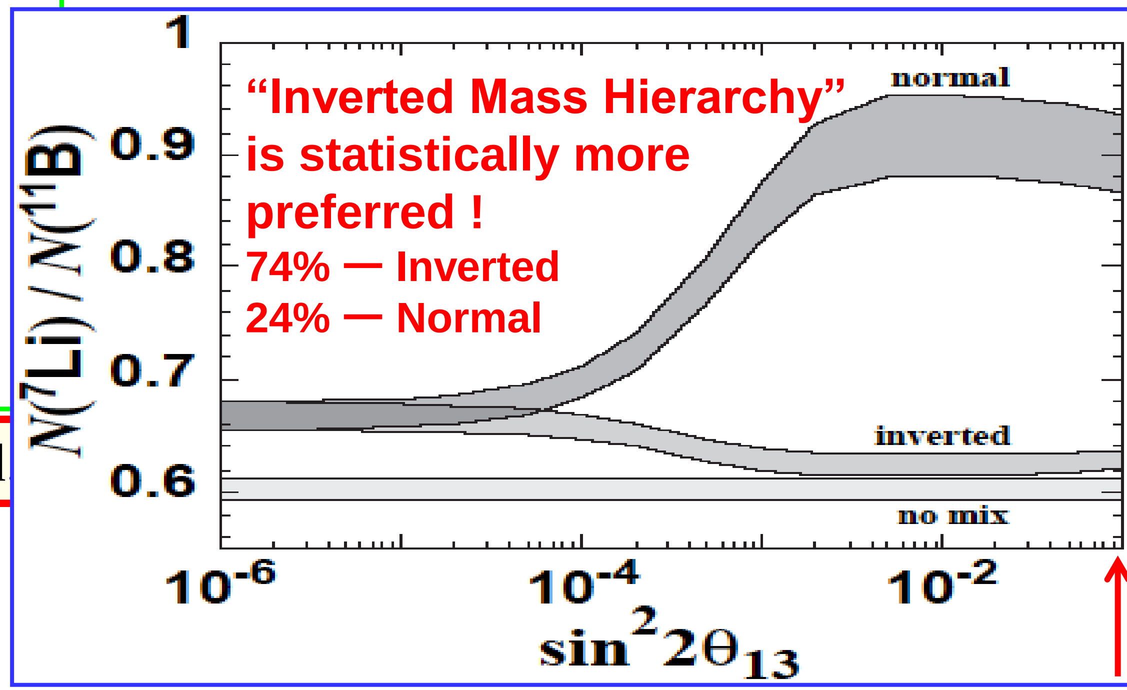

▪T2K, MINOS (2011)

▪Double CHOOZ, Daya Bay, RENO (2012)

$\sin^2 2\theta_{13} = 0.1$

Bayesian analysis:
Mathews, Kajino, Aoki and Fujiya, Phys. Rev. D85,105023 (2012).1

cf. Accelerator exp. → NH

Synthesis of ^{55}Mn in Pop.III Star

$^{56}Ni(\nu,\nu'p)^{55}Co, \quad ^{55}Co(e^-,\nu)^{55}Fe(e^-,\nu)^{55}Mn$

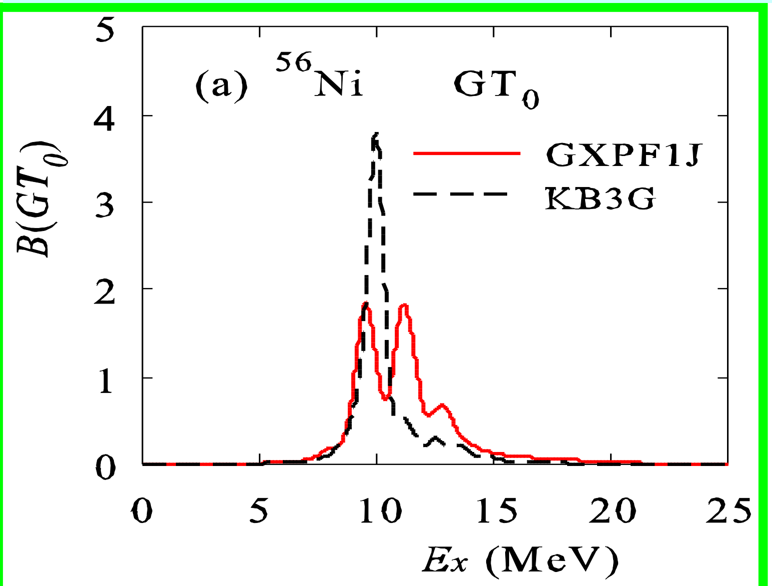

B(GT)=6.2
(GXPF1J)
B(GT)=5.4
(KB3G)

cf:
HW02
▲ gamma
● p
● n

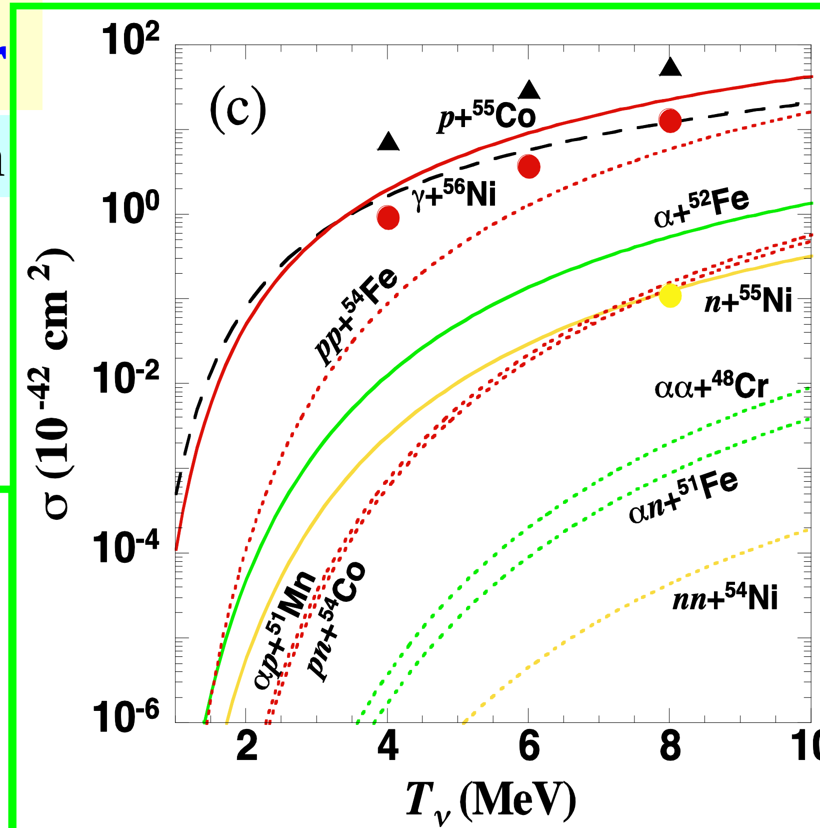

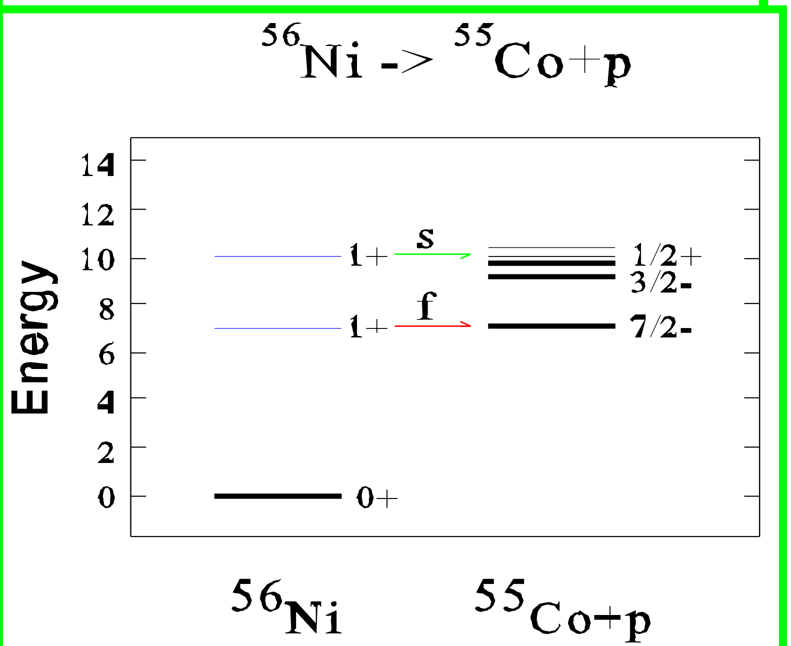

$^{54}Fe(p,\gamma)^{55}Co$

large proton emission cross section

Suzuki, Honma et al., PR C79, 061603(R) (2009)

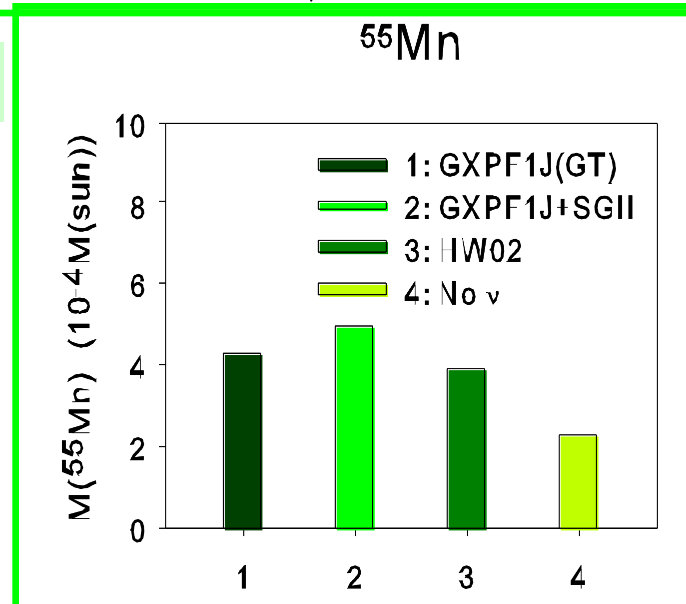

▪ ν- ^{40}Ar reactions

Liquid argon = powerful target for SNν detection

VMU= Monopole-based universal interaction

tensor force: bare≈renormalized

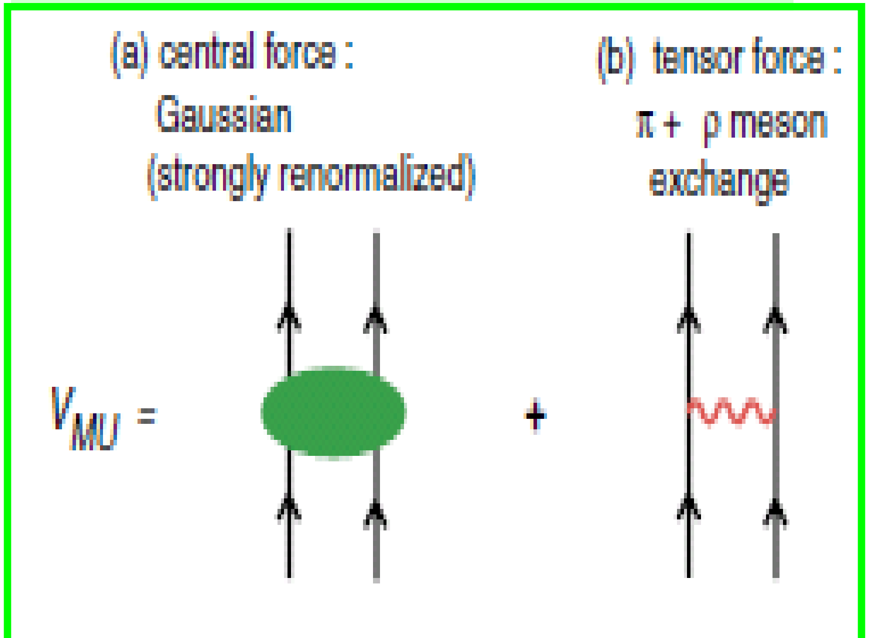

FIG. 2 (color online). Diagrams for the V_{MU} interaction.

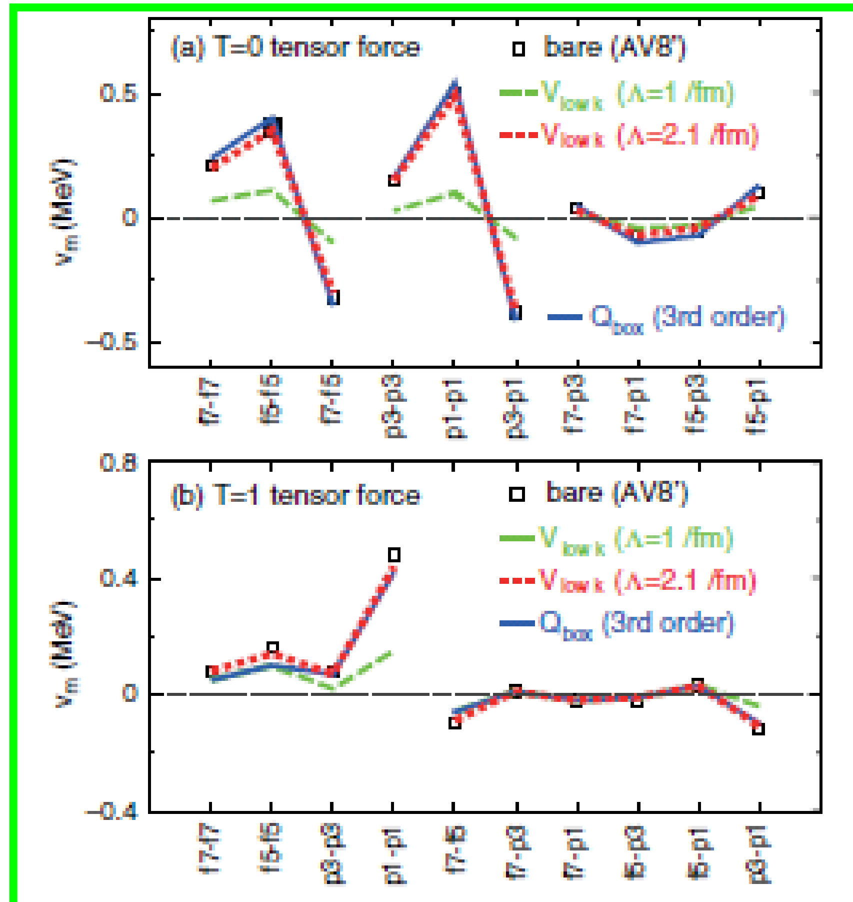

Important roles of tensor force

Otsuka, Suzuki, Honma, Utsuno,
Tsunoda, Tsukiyama, Hjorth-Jensen
PRL 104 (2010) 012501

▪ ν- ^{40}Ar reactions

Liquid argon = powerful target for SNν detection

sd-pf shell: **^{40}Ar (ν, e$^-$) ^{40}K** (sd)$^{-2}$ (fp)^2 : 2hw

SDPF-VMU-LS

sd: SDPF-M (Utsuno et al.) fp: GXPF1 (Honma et al.)

sd-pf: VMU + 2-body LS

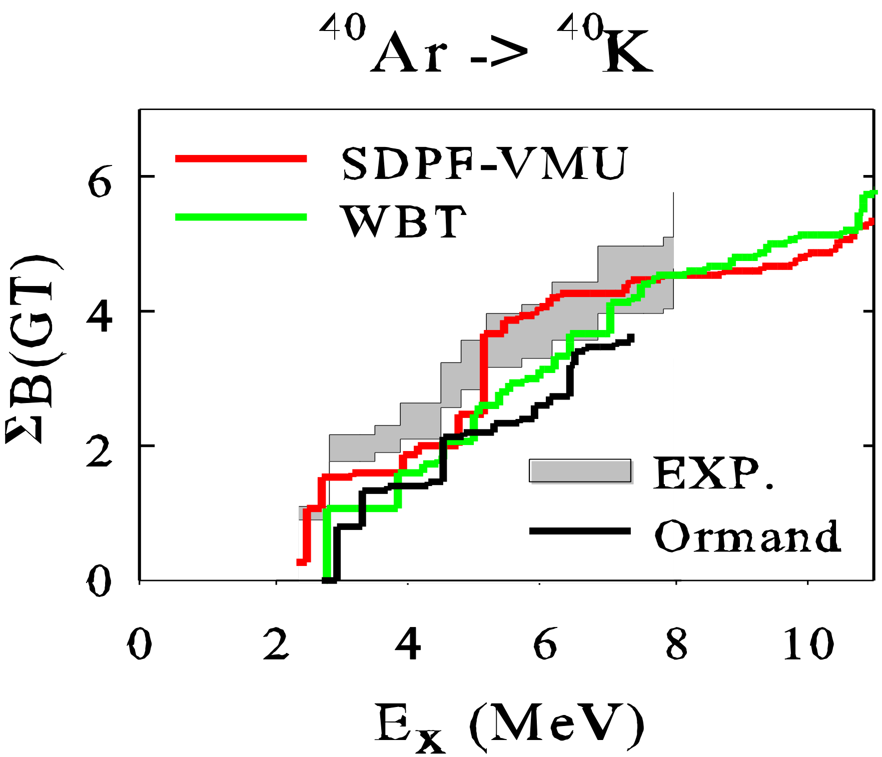

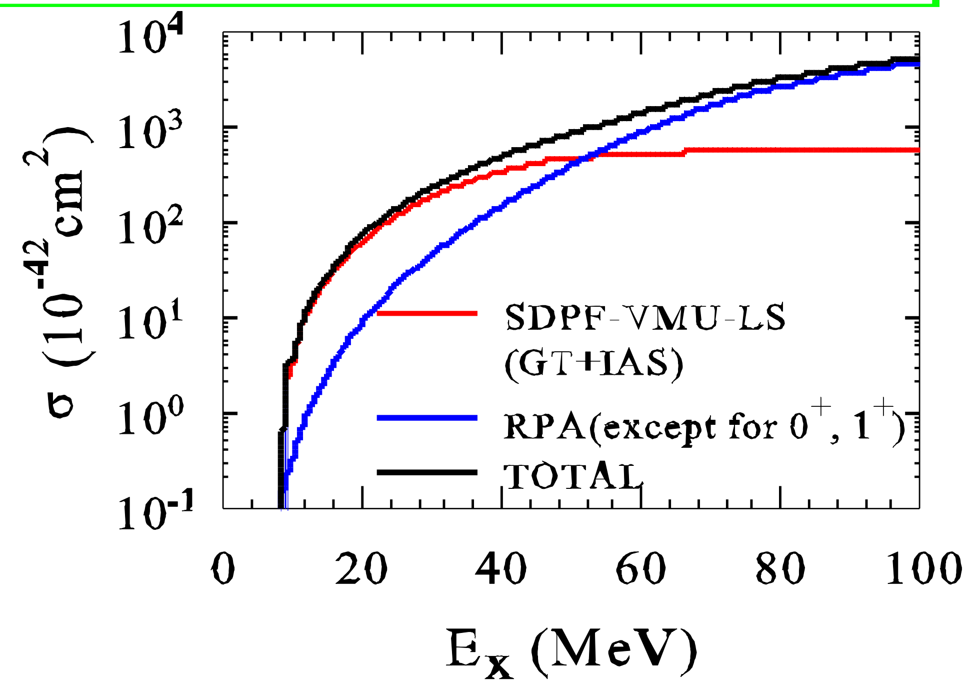

Suzuki and Honma, PR C87, 014607 (2013)
(p,n) Bhattacharya et al., PR C80, 055501 (2009)
Ormand et al, PL B345, 343 (1995); β-decay of ^{40}Ti

cf: E. Kolbe, K. Langanke, G. Martınez-Pinedo, and P. Vogel, J. Phys. G **29**, 2569 (2003);
I. Gil-Botella and A. Rubbia, JCAP **10**, 9 (2003).

Various roles of ν's in SN-nucleosynthesis

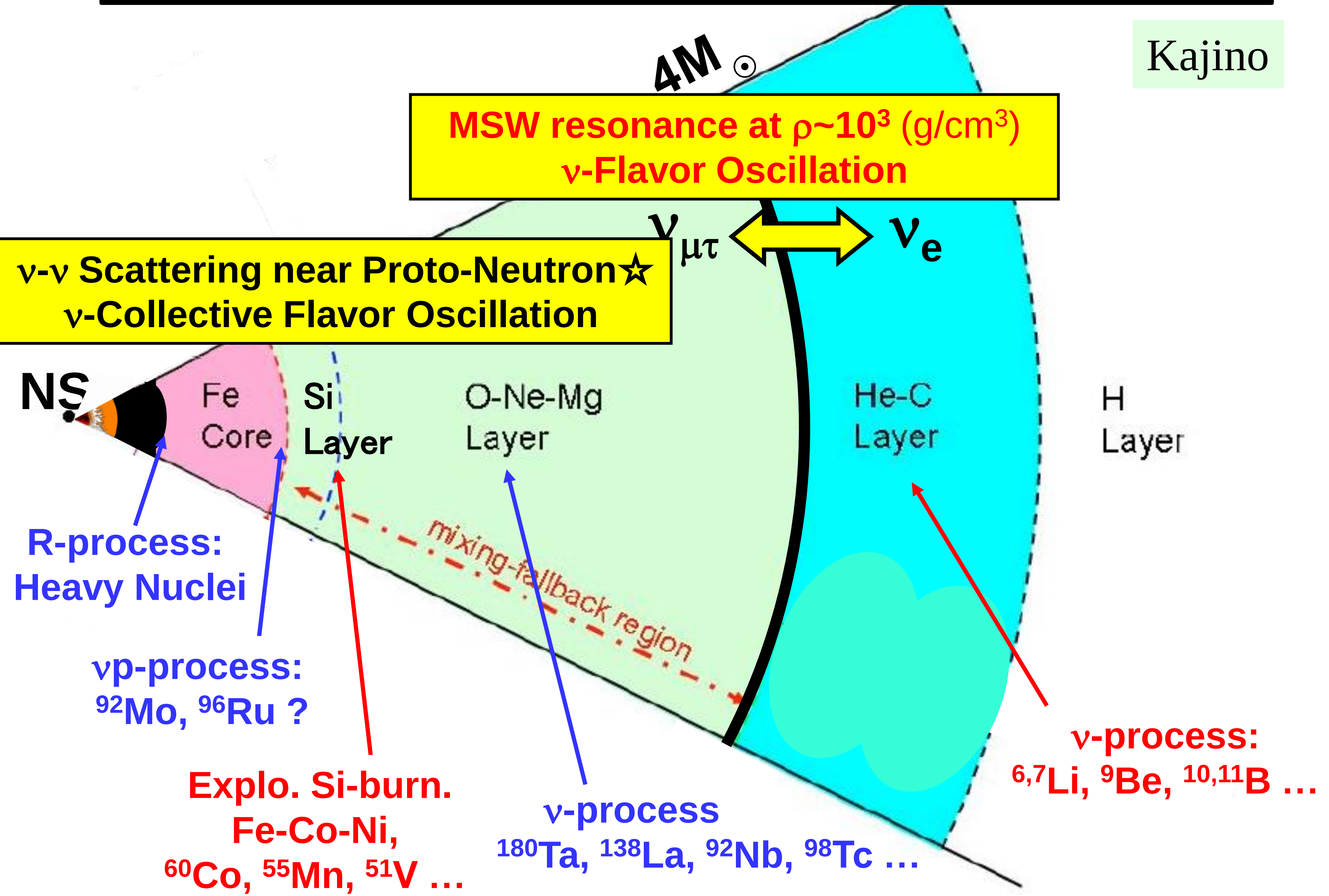

Spectrum with ν-oscillations

- With collective oscillation effects

G.G. Raffelt / Progress in Particle and Nuclear Physics 64 (2010) 393–399

$\langle E_{\nu_e}\rangle = 10$, $\langle E_{\bar{\nu}_e}\rangle = 14$ and $\langle E_{\nu_x}\rangle = 18$ MeV.

Normal

Inverted

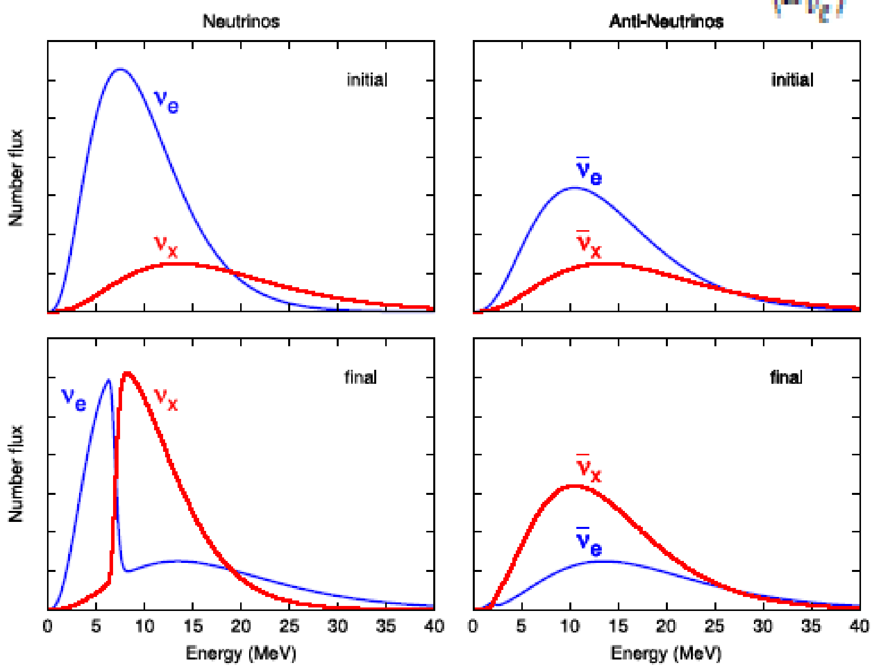

$$A: \quad F_{\nu_e}(E) = F_{\nu_x}(E)$$

B:

$$F_{\nu_e}(E) = \sin^2\theta_{12} F_{\nu_e}(E)$$

$$+ \cos^2\theta_{12} F_{\nu_x}(E) \quad (E < E_{split})$$

$$F_{\nu_e}(E) = F_{\nu_x}(E) \quad (E > E_{split})$$

- With collective and MSW effects

$$F_{\bar{\nu}_e}(E) = \bar{p}(E) F^0_{\bar{\nu}_e}(E) + [1 - \bar{p}(E)] F^0_{\bar{\nu}_x}(E),$$

Survival probabilities including collective effects for the scenario described in the text.

Scenario	Hierarchy	$\sin^2\Theta_{13}$	$p(E < E_{split})$	$p(E > E_{split})$	$\bar{p}(E)$	Earth effects
A	Normal	$\gtrsim 10^{-3}$	0	0	$\cos^2\Theta_\odot$	$\bar{\nu}_e$
B	Inverted	$\gtrsim 10^{-3}$	$\sin^2\Theta_\odot$	0	$\cos^2\Theta_\odot$	$\bar{\nu}_e$
C	Normal	$\lesssim 10^{-5}$	$\sin^2\Theta_\odot$	$\sin^2\Theta_\odot$	$\cos^2\Theta_\odot$	ν_e and $\bar{\nu}_e$
D	Inverted	$\lesssim 10^{-5}$	$\sin^2\Theta_\odot$	0	0	–

Cross sections folded over the spectra

- Target = ^{13}C

$\langle E_{\nu_e}\rangle = 10,\ \langle E_{\bar{\nu}_e}\rangle = 14$ and $\langle E_{\nu_x}\rangle = 18$ MeV.

$E_\nu \le 10\text{MeV} \quad E_\nu^{th}(^{12}C) \approx 13\text{MeV}$

Natural isotope abund. = 1.07%

	A (normal)	B (inverted)
no oscillation	8.01	8.01 ($10^{-42}cm^2$)
collective osc.	8.01	39.44 (39.93)
collective +MSW	39.31	39.35 (39.53)

- Target = ^{48}Ca $Q(^{48}Ca-^{48}Sc)=2.8$ MeV $E(1^+;\ ^{48}Sc) = 2.5$ MeV

	A (normal)	B (inverted)
no oscillation	73.56	73.56 ($10^{-42}cm^2$)
collective osc.	73.56	303.4
collective +MSW	302.6	302.8

Cross sections are enhanced by oscillations.

E_{split} is too small to distinguish the ν-mass hierarchy in case of Collect.+MSW oscillations ( ): E_{split} =15 MeV

Electron-capture (weak) rates in stellar environments

- standard rates available

Sullivan et al., ApJ. 816, 44 (2016)

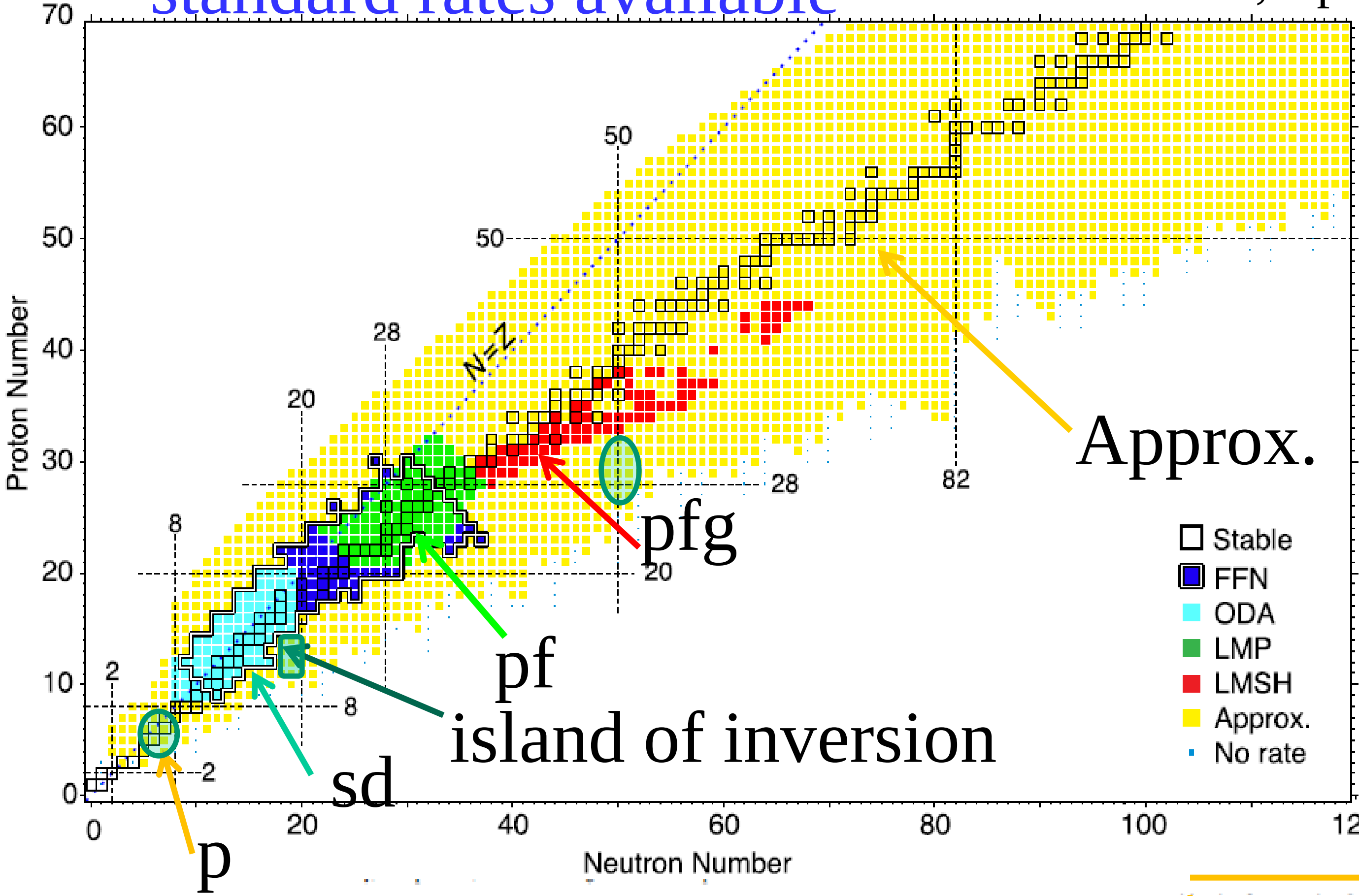

- Missing
- Island of inv. sd-pf
- ~^{78}Ni N=50 pf-gds
- p-shell

Approx.

B (=4.6) and ΔE (=2.5 MeV)

$$\eta = \chi + \mu_e/T,$$

$$\chi = (Q - \Delta E)/T,$$

$$\lambda_{EC} = \frac{\ln 2 \cdot B}{K}\left(\frac{T}{m_e c^2}\right)^5 \left[F_4(\eta) - 2\chi F_3(\eta) + \chi^2 F_2(\eta)\right]$$

$$F_k(\eta) = \int_0^\infty \frac{x^k}{\exp(x-\eta)+1} dx,$$

$$F_k(\eta) = -\Gamma(k+1)\mathrm{Li}_{k+1}(-e^\eta),$$

Table	Model Space					T (GK)	$\mathrm{Log}_{10}(\rho Y_e$ g cm$^{-3})$	Reference
	s	p	sd	pf	pfg/sdg			
FFN	x	...	x	x	...	0.01–100	1.0–11	Fuller et al. (1982)
ODA	x	...	x	...	...	0.01–30	1.0–11	Oda et al. (1994)
LMP	x	...	...	x	...	0.01–100	1.0–11	Langanke et al. (2003), Langanke (2001a)
LMSH	...	...	...	...	x	8.12–39.1	9.22–12.4	Hix et al. (2003), Langanke et al. (2001a)
Approx.	x	x	x	x	x	...	...	Langanke et al. (2003)

▪ Weak Rates in sd-shell and Nuclear URCA process in O-Ne-Mg cores

- $M = 8M_\odot \sim 10M_\odot$

  C burning → O-Ne-Mg core

  → (1) O-Ne-Mg white dwarf (WD)

  → (2) e-capture supernova explosion (collapse of O-Ne-Mg core induced by e-capture) with neutron star (NS) remnant

  → (3) core-collapse (iron-core collapse) supernova explosion with NS (neon burning shell propagates to the center)

Fate of the star is sensitive to its mass and nuclear e-capture and β–decay rates; Cooling of O-Ne-Mg core by nuclear URCA processes determines (2) or (3).

Nomoto and Hashimoto, Phys. Rep. 163, 13 (1988)
Miyaji, Nomoto, Yokoi, and Sugimoto, Pub. Astron. Soc. Jpn. 32, 303 (1980)
Nomoto, Astrophys. J. 277, 791 (1984); ibid. 322, 206 (1987)

- URCA processes in sd-shell nuclei

→ Cooling of O-Ne-Mg core in 8-10 $M_\odot$ stars

e-capture: $^{A}_{Z}X + e^- \to {}_{Z-1}^{A}Y + \nu$

β-decay: ${}_{Z-1}^{A}Y \to {}^{A}_{Z}X + e^- + \bar{\nu}$

They occur simultaneously at certain stellar conditions and energy is lost from stars by emissions of ν and $\bar{\nu}$ → Cooling of stars

How much star is cooled → fate of the star after neon flash:

$$^{23}Na + e^- \to {}^{23}Ne + \nu$$
$$^{23}Ne \to {}^{23}Na + e^- + \bar{\nu}$$
$$^{25}Mg + e^- \to {}^{25}Na + \nu$$
$$^{25}Na \to {}^{25}Mg + e^- + \bar{\nu}$$
$$^{27}Al + e^- \to {}^{27}Mg + \nu$$
$$^{27}Mg \to {}^{27}Al + e^- + \bar{\nu}$$

A=23: Q=4.376 MeV
A=25: Q=3.835 MeV
A=27: Q=2.610 MeV

- Beta-decay Q-values

Odd-A sd-shell Nuclei (A=17-31)

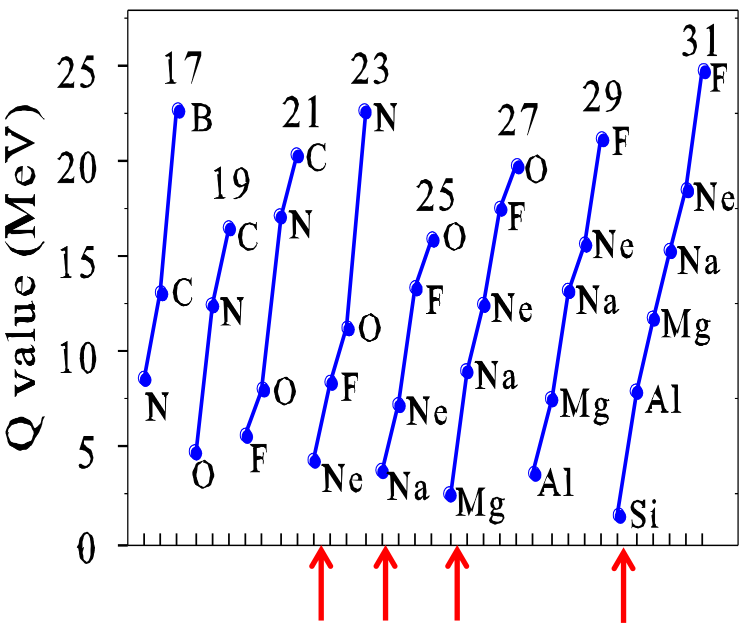

Electron chemical potential

TABLE III. Electron chemical potential μ_e (in units of MeV) at high densities, $\rho Y_e = 10^7$–10^{10} g/cm^3, and high temperatures, $T = T_9 \times 10^9$ K.

ρY_e (g/cm^3)	T_9									
	1	2	3	4	5	6	7	8	9	10
10^7	1.200	1.133	1.021	0.870	0.698	0.534	0.404	0.310	0.244	0.196
10^8	2.437	2.406	2.355	2.283	2.192	2.081	1.952	1.808	1.653	1.493
10^9	5.176	5.162	5.138	5.105	5.062	5.010	4.948	4.877	4.797	4.708
10^{10}	11.116	11.109	11.098	11.083	11.063	11.039	11.011	10.978	10.940	10.898

▪ Nuclear weak rates in sd-shell

(1) New shell-model Hamiltonian: USDB   cf. Oda et al., USD

(2) Fine meshes in both density and temperature

($\Delta\log_{10}(\rho Ye)=0.02$, $\Delta \log_{10}T=0.05$)

cf. Interpolation problem in FFN (Fuller-Fowler-Newman) grids

FFN grids are rather scarce, especially for the density

(3) Effects of screening   Suzuki, Toki and Nomoto, ApJ. 817, 163 (2016)

(^{23}Ne, ^{23}Na)

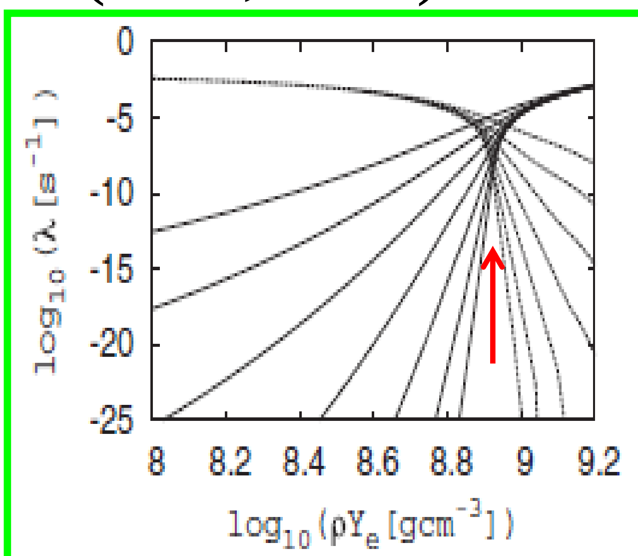

URCA density at

$\log_{10}\rho Y_e = 8.92$

(^{25}Na, ^{25}Mg)

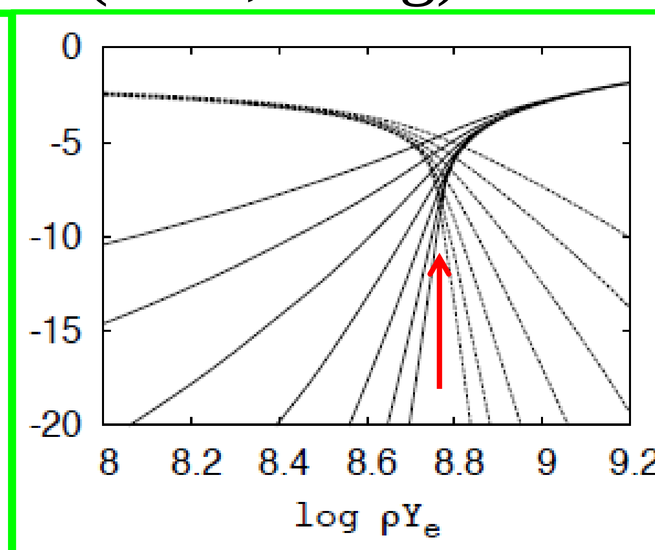

URCA density at

$\log_{10}\rho Y_e = 8.78$

(^{27}Mg, ^{27}Al)

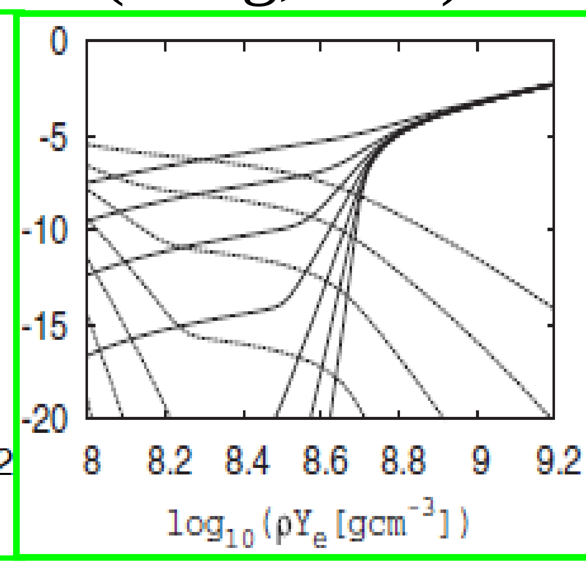

g.s. $1/2^+ \longleftrightarrow 5/2^+$ forbidden

No clear URCA density for A=27 pair

Cooling of O-Ne-Mg core by the nuclear URCA processes

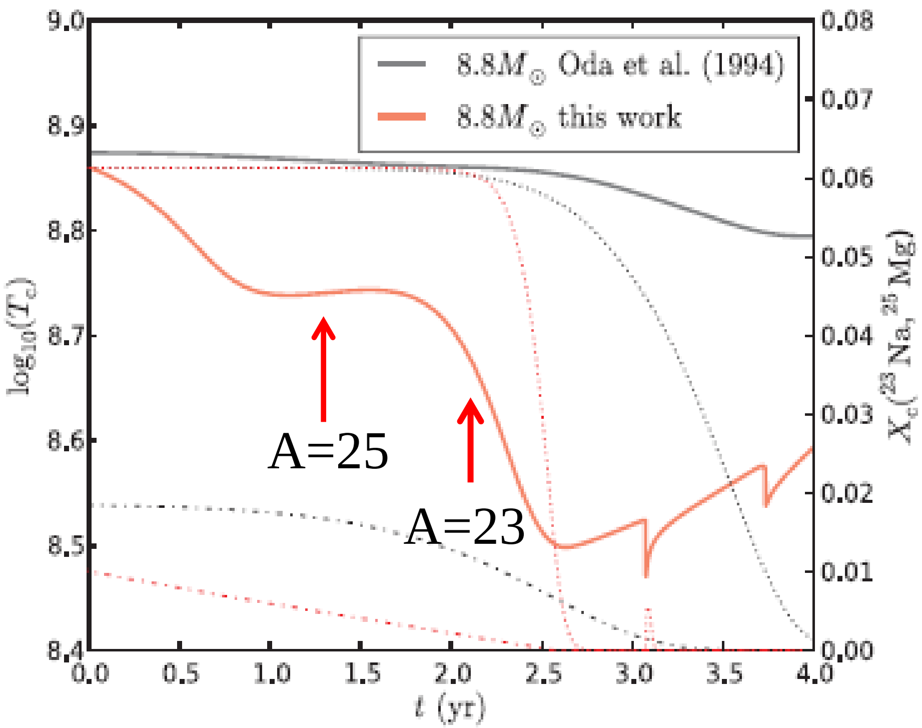

8.8$M_\odot$ star collapses triggered by subsequent e-capture on ^{24}Mg and ^{20}Ne (e-capture supernova explosion)

Toki, Suzuki, Nomoto, Jones and Hirschi, PR C 88, 015806 (2013)

Fate of 8-10$M_\odot$ stars

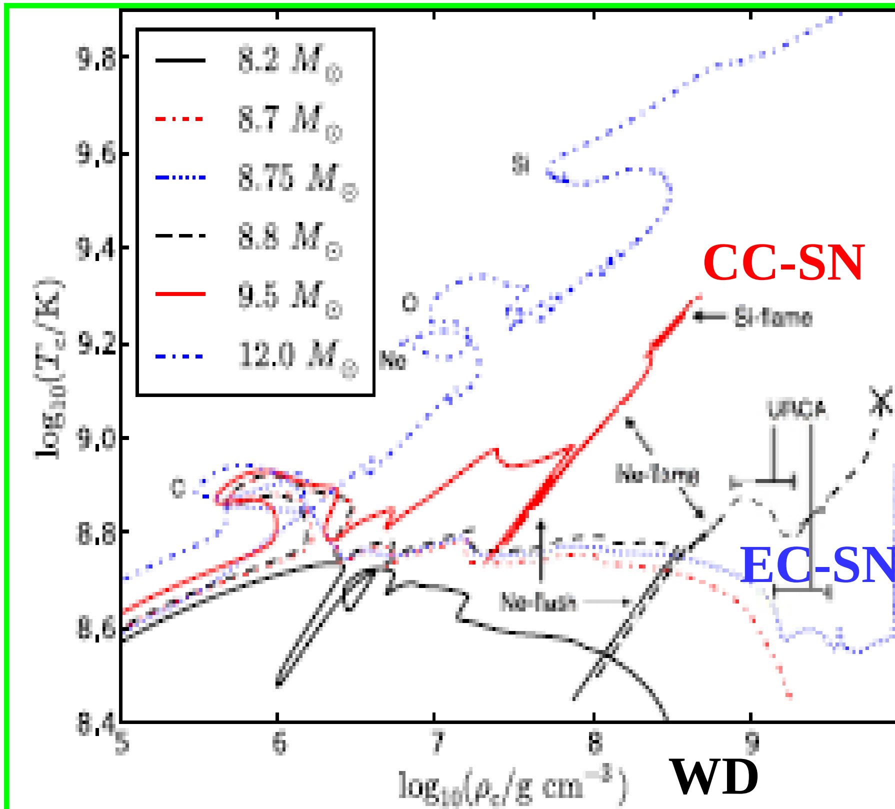

Border of CC-SN or EC-SN is at M∼9$M_\odot$, which is quite sensitive to nuclear weak rates

Jones et al., Astrophys. J. 772, 150 (2013)

Ab-initio effective sd-shell interactions from chiral NN (N^3LO) and 3N (N^2LO)

・IM-SRG (in-medium similarity renormalization group)

Stroberg et al., PRC 93 (2016) ; Tsukiyama, Bogner and Schwenk, PRL 106 (2011)

Hamiltonian H, which is normal ordered with respect to a finite-density reference state $|\Phi\rangle$ (e.g., the Hartree-Fock ground state) is given as

$$H = E_0 + \sum_{ij} f_{ij}\{a_i^\dagger a_j\} + \frac{1}{2!^2}\sum_{ijkl}\Gamma_{ijkl}\{a_i^\dagger a_j^\dagger a_l a_k\} + \frac{1}{3!^2}\sum_{ijklmn} W_{ijklmn}\{a_i^\dagger a_j^\dagger a_k^\dagger a_n a_m a_l\},$$

where E_0, f_{ij}, Γ_{ijkl}, and W_{ijklmn} are the normal-ordered zero-, one-, two-, and three-body terms, respectively [44]. The

$$H(s) = U(s)HU^\dagger(s) \equiv H^d(s) + H^{od}(s). \qquad (2)$$

Here, $H^d(s)$ is the diagonal part and $H^{od}(s)$ is the off-diagonal part of the Hamiltonian. As $s \to \infty$, the off-diagonal matrix elements become zero.

$$\frac{dH(s)}{ds} = [\eta(s), H(s)], \quad \eta(s) \equiv \frac{dU(s)}{ds}U^\dagger(s).$$

・CCEI (coupled-cluster effective interaction) Jansen et al, PRC 94 (2016)

$$\hat{H}_A = \sum_{i<j}\left(\frac{(\mathbf{p}_i - \mathbf{p}_j)^2}{2mA} + \hat{V}_{NN}^{(i,j)}\right) + \sum_{i<j<k}\hat{V}_{3N}^{(i,j,k)}.$$

$$H_{\rm CCEI}^A = H_0^{A_c} + H_1^{A_c+1} + H_2^{A_c+2} + \cdots . \qquad (6)$$

Here the first term $H_0^{A_c}$ stands for the core, the second term $H_1^{A_c+1}$ for the valence one-body, and $H_2^{A_c+2}$ for the two- body Hamiltonian. The two-body term is derived from

$$[S^\dagger S]^{1/2}\hat{H}_{\rm CCEI}^A[S^\dagger S]^{-1/2}.$$

Energies (g.s. and excited states) of O, F, Ne, Mg isotopes are well described.

GT strtength with ab initio interactions
IM-SRG & CCEI vs USDB

Saxena, Srivastava and Suzuki,
PRC97, 024310 (2018)

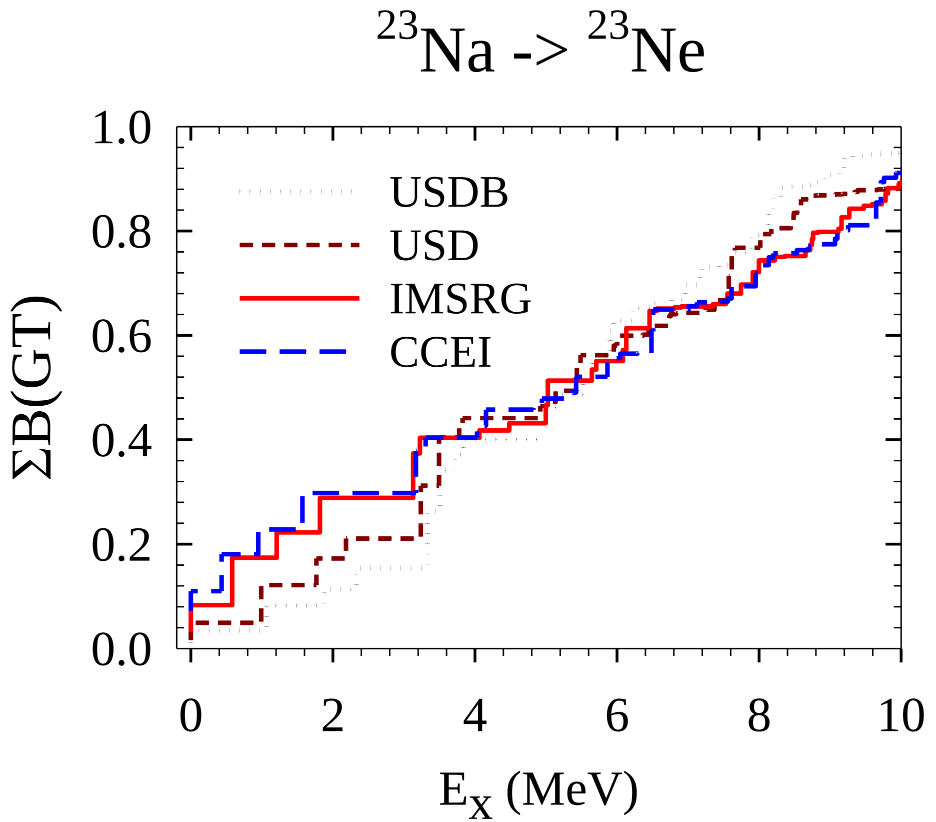

$q_{GT} = 0.77$

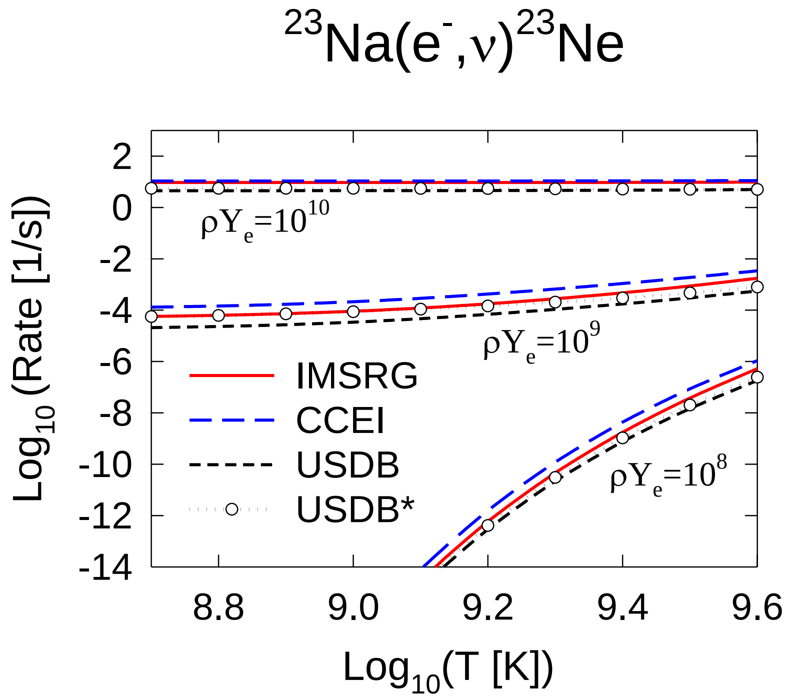

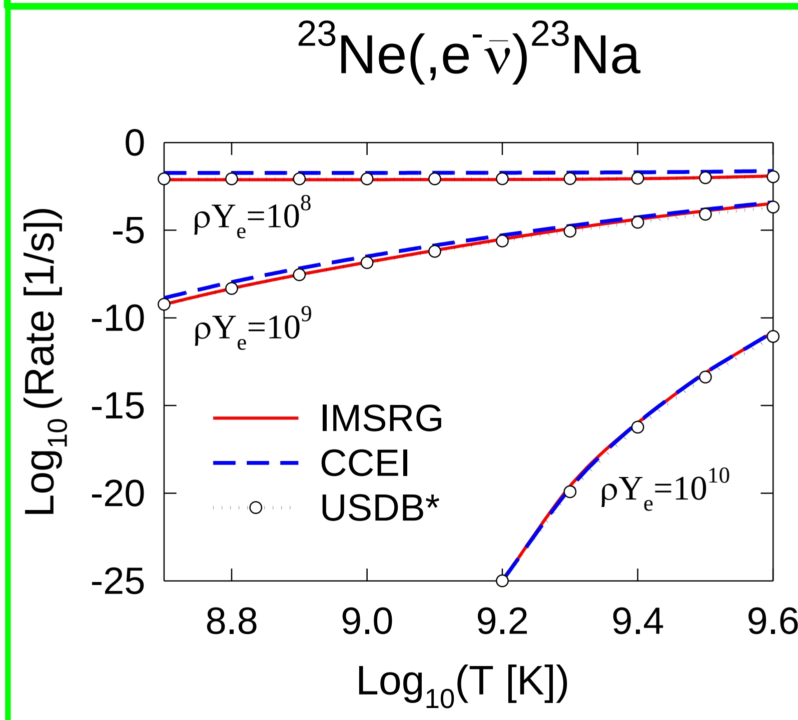

$B(GT)_{eff}$ vs $B(GT)_{exp}$ for beta-decays in T=1/2 mirror sd-shell nuclei

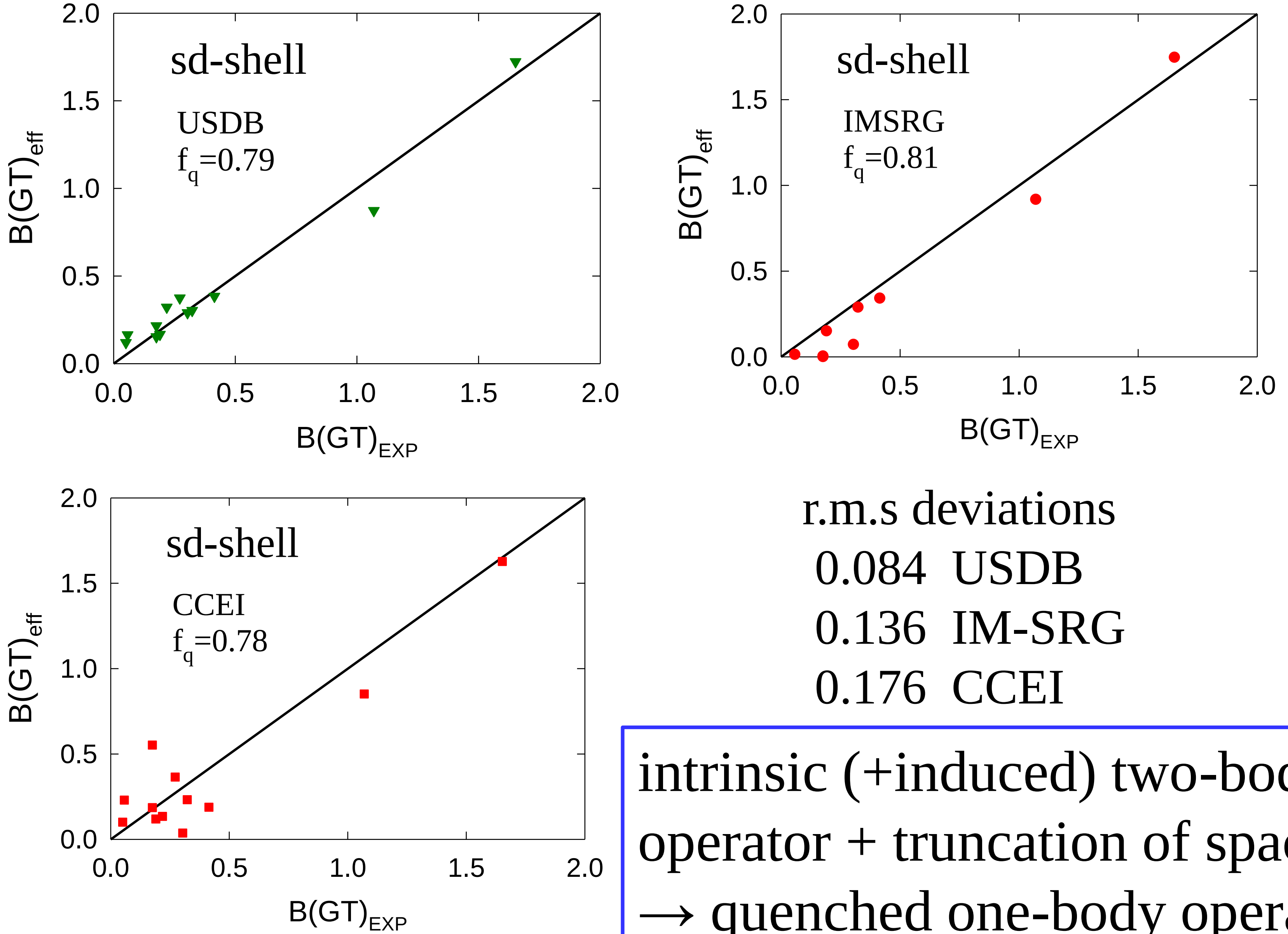

r.m.s deviations

0.084 USDB

0.136 IM-SRG

0.176 CCEI

intrinsic (+induced) two-body operator + truncation of space → quenched one-body operator

ESPE (neutron)

CCEI

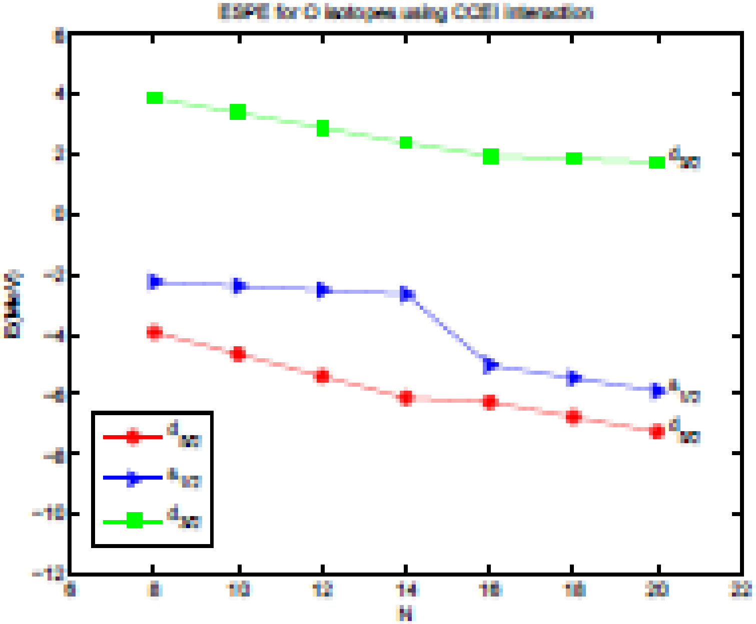

USDB

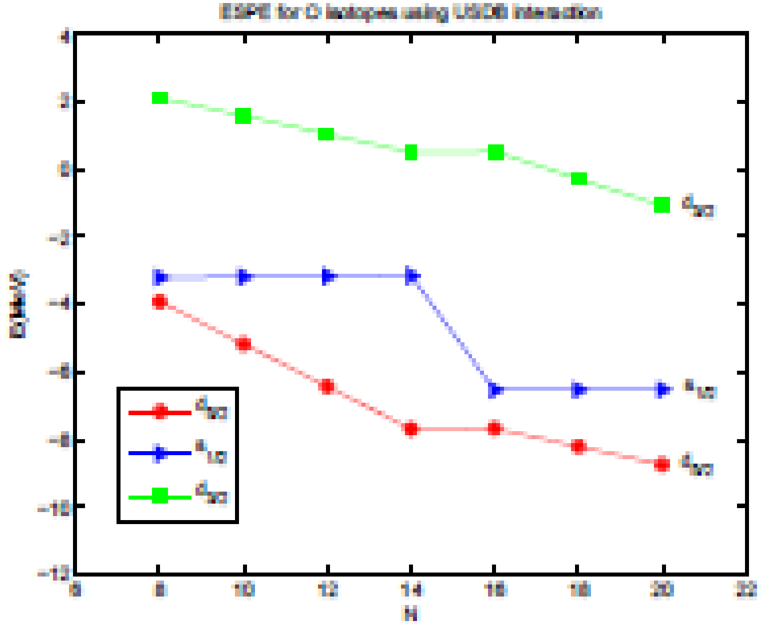

▪pf-shell: GT strength in ^{56}Ni: GXPF1J vs KB3G vs KBF

KBF: Table by Langanke and Martinez-Pinedo,

At. Data and Nucle. Data Tables 79, 1 (2001)

- fp-shell nuclei: KBF   Caurier et al., NP A653, 439 (1999)
- Experimental data available are taken into account: Experimantal Q-values, energies and B(GT) values available
- Densities and temperatures at FFN (Fuller-Fowler-Newton)   grids:

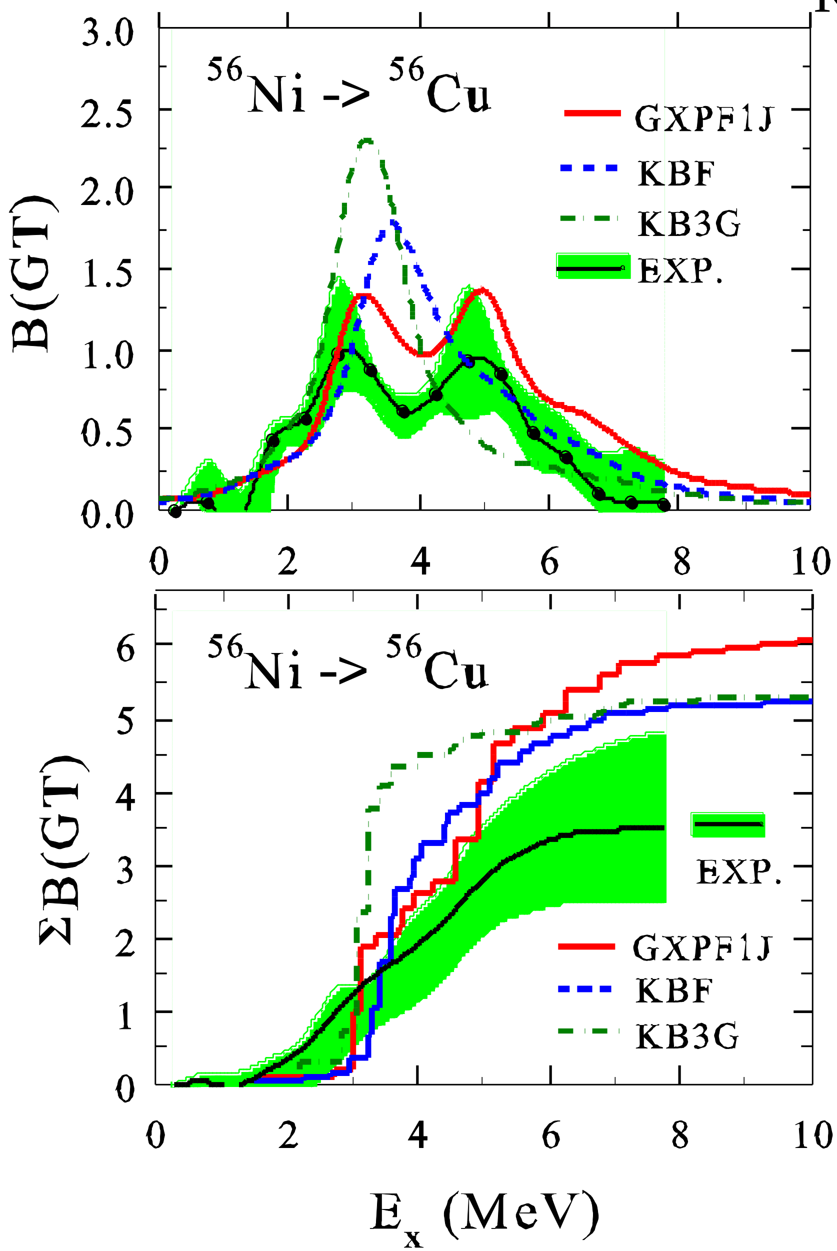

EXP: Sasano et al., PRL 107, 202501 (2011)

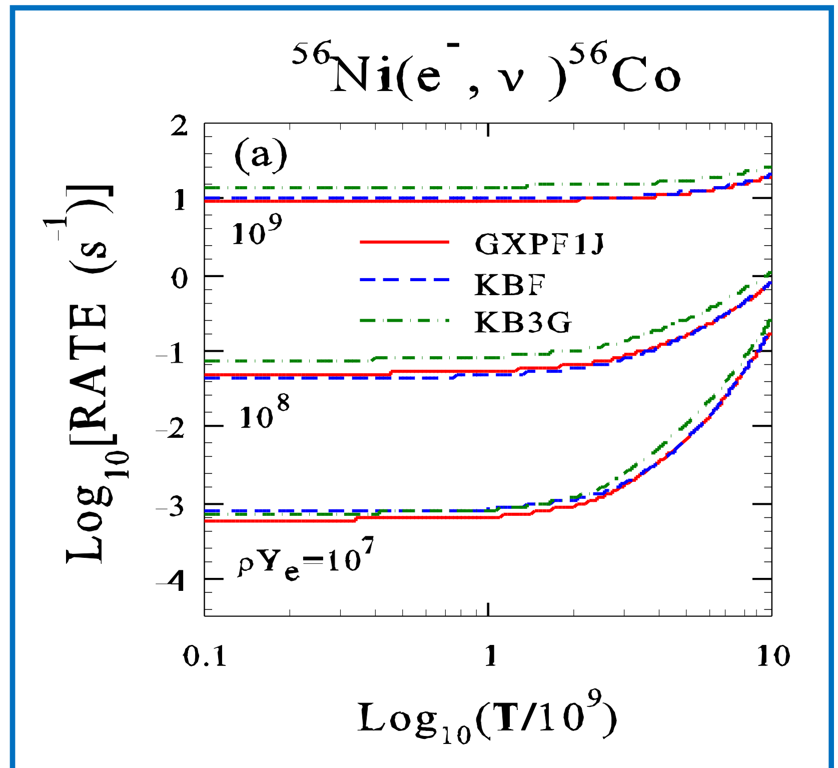

・Type-Ia SNe and synthesis of iron-group nuclei

Accretion of matter to white-dwarf from binary star

→ supernova explosion when white-dwarf mass ≈ Chandrasekhar limit

→ ^{56}Ni (N=Z)

→ ^{56}Ni (e$^-$, ν) ^{56}Co Y_e =0.5 → Y_e < 0.5 (neutron-rich)

→ production of neutron-rich isotopes; more ^{58}Ni

Decrease of e-capture rate on ^{56}Ni →less production of ^{58}Ni and larger Y_e

Problem of over-production of neutron-excess iron-group isotopes such as ^{58}Ni, ^{54}Cr … compared with solar abundances

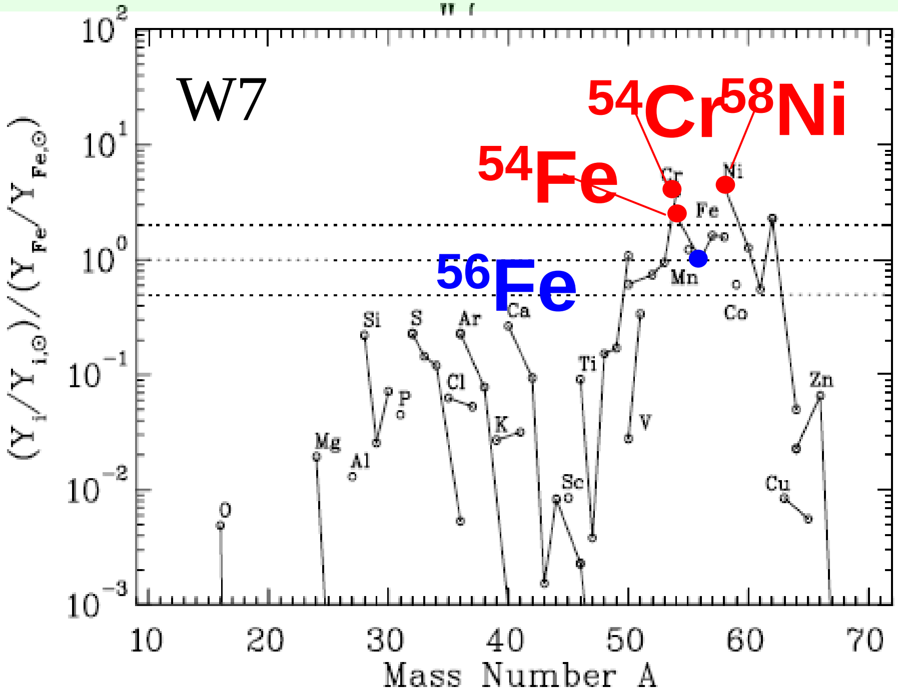

Iwamoto et al., ApJ. Suppl, 125, 439 (1999)

e-capture rates with FFN (Fuller-Fowler-Newman)

Type-Ia SNe

W7 model: fast deflagration

WDD2: Slow deflagration + delayed detonation

Initial: C-O white dwarf, $M=1.0M_\odot$

central; ρ_9=2.12, T_c=1x10^{7}K

e-capture rates: GXP; GXPF1J (21≤Z≤32) and KBF (other Z)

GXP
W7

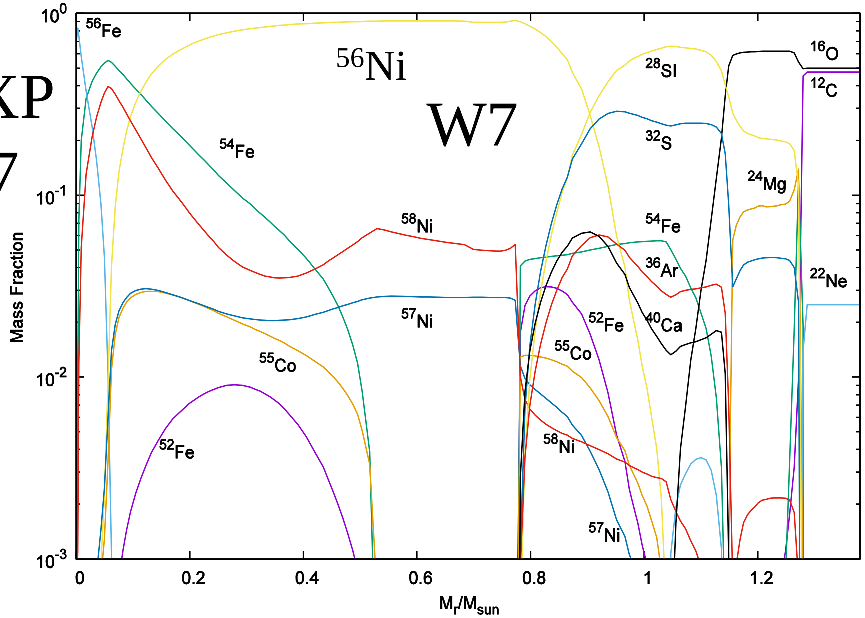

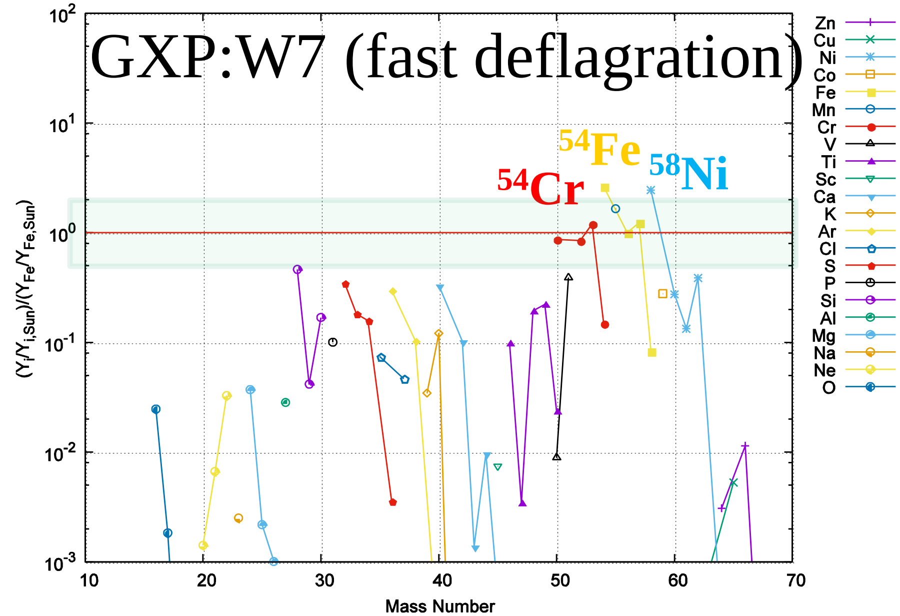

GXP: WDD2 (slow deflagration + detonation)

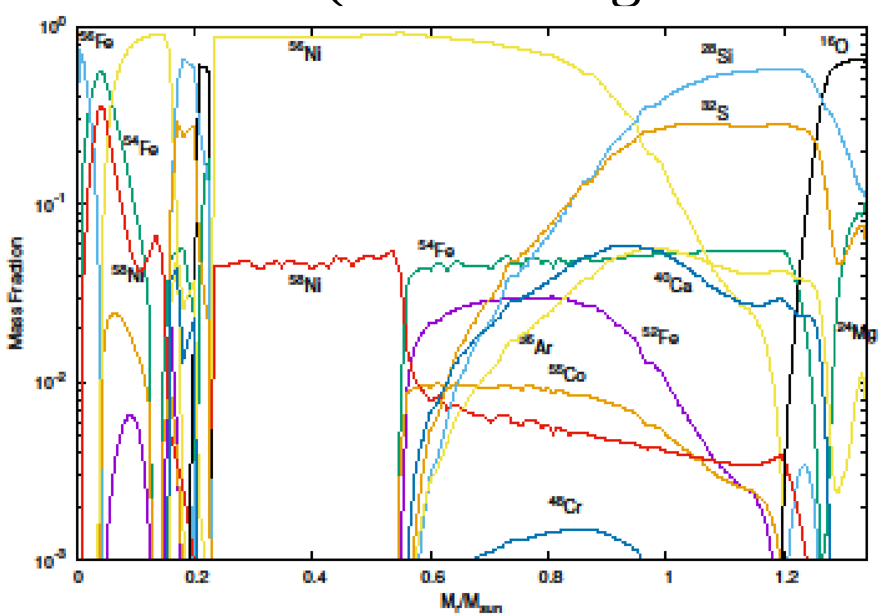

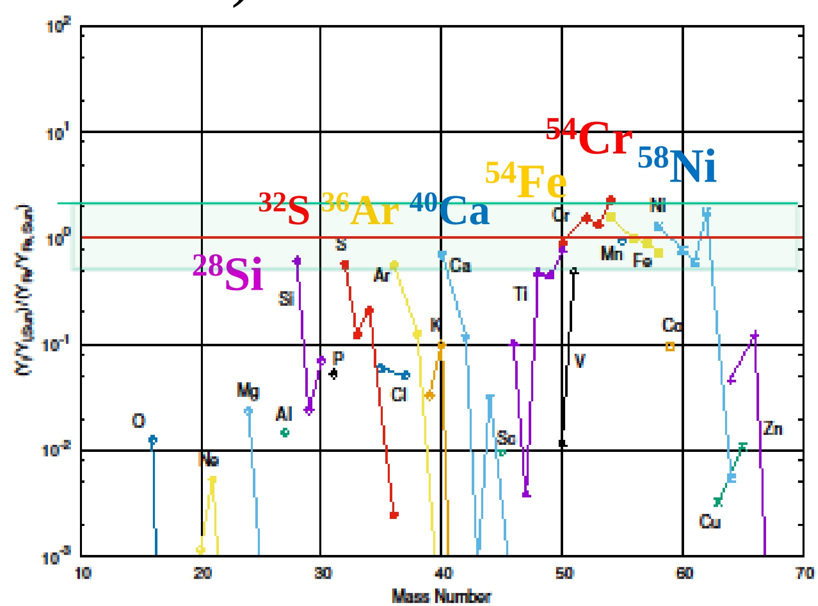

Mori, Famiano, Kajino, Suzuki, Hidaka, Honma, Iwamoto, Nomoto, Otsuka, ApJ. 833, 179 (2016)

▪Weak rates for nuclei in the island of inversion

Nature 505, 65 (2014)
doi:10.1038/nature12757

Strong neutrino cooling by cycles of electron capture and β^- decay in neutron star crusts

H. Schatz[1,2,3], S. Gupta[4], P. Möller[2,5], M. Beard[2,6], E. F. Brown[1,2,3], A. T. Deibel[2,3], L. R. Gasques[7], W. R. Hix[8,9], L. Keek[1,2,3], R. Lau[1,2,3], A. W. Steiner[2,10] & M. Wiescher[2,6]

Rates evaluated by QRPA
Shell-model evaluations are missing.

Table 1 | Electron-capture/β^--decay pairs with highest cooling rates

Electron-capture/β^--decay pair		Density†	Chemical potential†	Luminosity‡
Parent	Daughter*	(10^{10} g cm^{-3})	(MeV)	(10^{36} erg s^{-1}
^{29}Mg	^{29}Na	4.79	13.3	24
^{55}Ti	^{55}Sc, ^{55}Ca	3.73	12.1	11
^{31}Al	^{31}Mg	3.39	11.8	8.8
^{33}Al	^{33}Mg	5.19	13.4	8.3
56Ti	56Sc	5.57	13.8	3.5
^{57}Cr	^{57}V	1.22	8.3	1.6
^{57}V	^{57}Ti, ^{57}Sc	2.56	10.7	1.6
^{63}Cr	^{63}V	6.82	14.7	0.97
^{105}Zr	^{105}Y	3.12	11.2	0.92
^{59}Mn	^{59}Cr	0.945	7.6	0.88
^{103}Sr	^{103}Rb	5.30	13.3	0.65
^{96}Kr	^{96}Br	6.40	14.3	0.65
^{65}Fe	^{65}Mn	2.34	10.3	0.60
^{65}Mn	^{65}Cr	3.55	11.7	0.46

Island of inversion
Z=10-12, N = 20-22

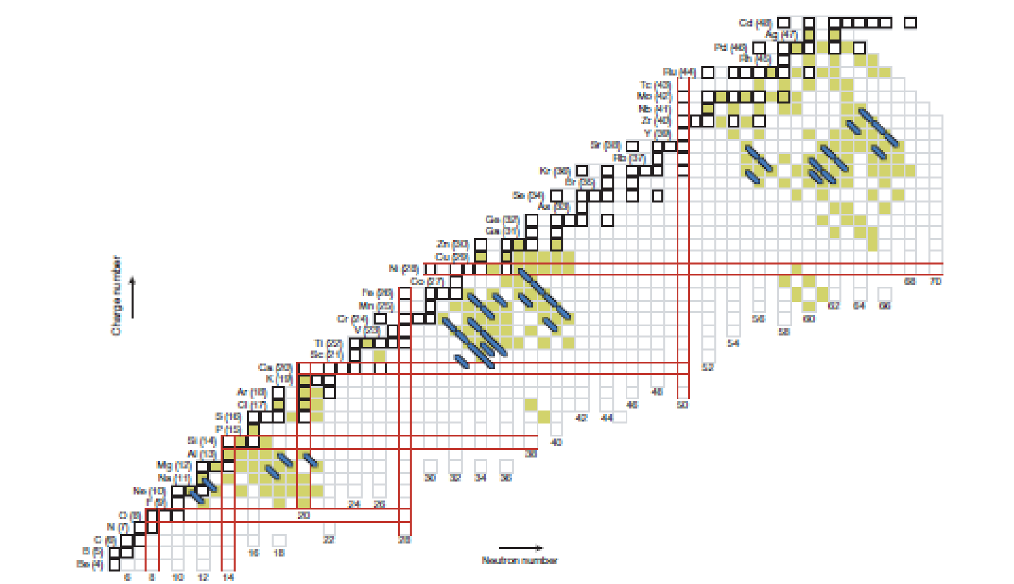

Figure 2 | Electron-capture/β^--decay pairs on a chart of the nuclides. The thick blue lines denote electron-capture/β^--decay pairs that would generate a strong neutrino luminosity in excess of 5×10^{34} erg s^{-1} at $T = 0.51$ GK for a composition consisting entirely of the respective electron-capture/β^--decay pair. They largely coincide with regions where allowed electron-capture and β^--decay transitions are predicted to populate low-lying states and subsequent electron capture is blocked (shaded squares, see also the discussion in ref. 3). These are mostly regions between the closed neutron and proton shells (pairs of horizontal and vertical red lines), where nuclei are significantly deformed (see Supplementary Information section 4). Nuclides that are β^--stable under terrestrial conditions are shown as squares bordered by thicker lines. Nuclear charge numbers are indicated in parentheses next to element symbols.

Island of inversion: sd<->pf

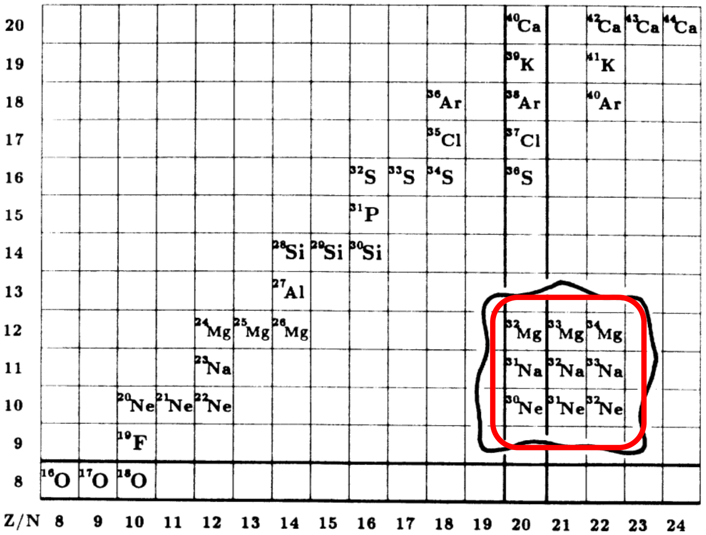

Warburton, Becker, Brown, PR C41, 1147 (1990)

- Small shell-gap: $f_{7/2}$-$d_{3/2}$
- Small $E_x(2^+)$
- Large B(E2)

→ Large sd-pf admixture

Neutron-rich Ne, Na, Mg isotopes

SDPF-M: Utsuno et al., PR C60, 054315 (1999)

# of nucleons in pf-shell

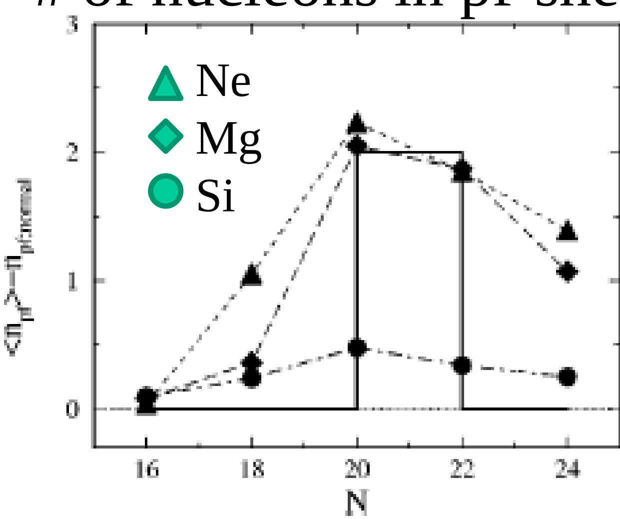

Neutron ESP for N=20 isotones

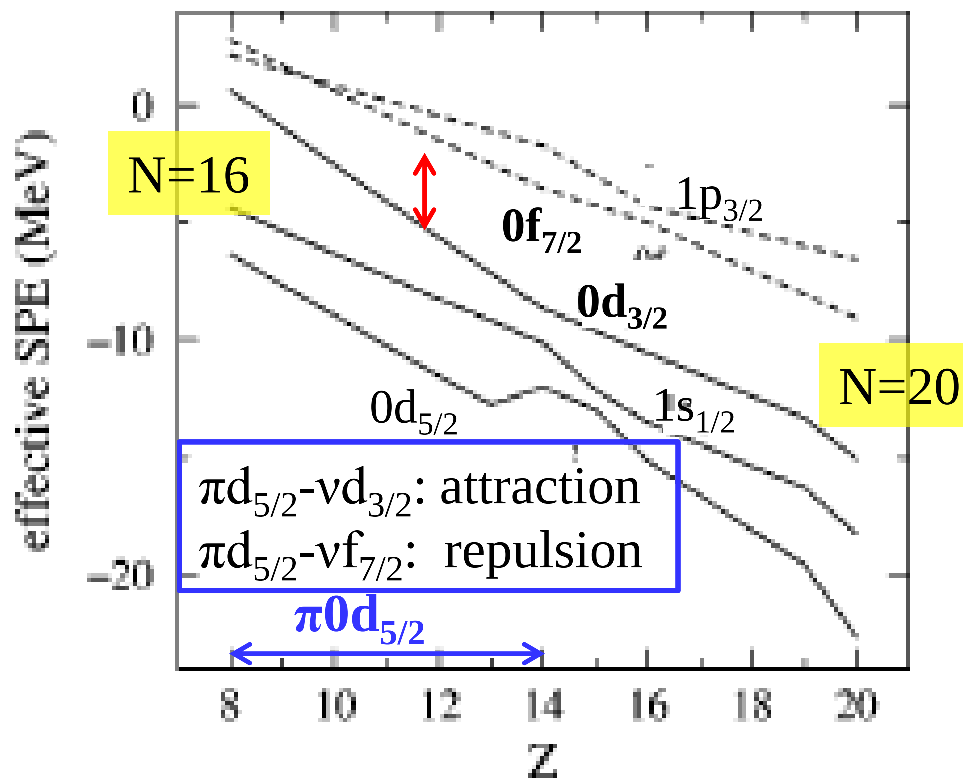

Shell-gap ($\nu d_{3/2}$-$\nu f_{7/2}$) decreases for less protons in $d_{5/2}$-shell → Magic number changes from N=20 to N=16

^{31}Mg

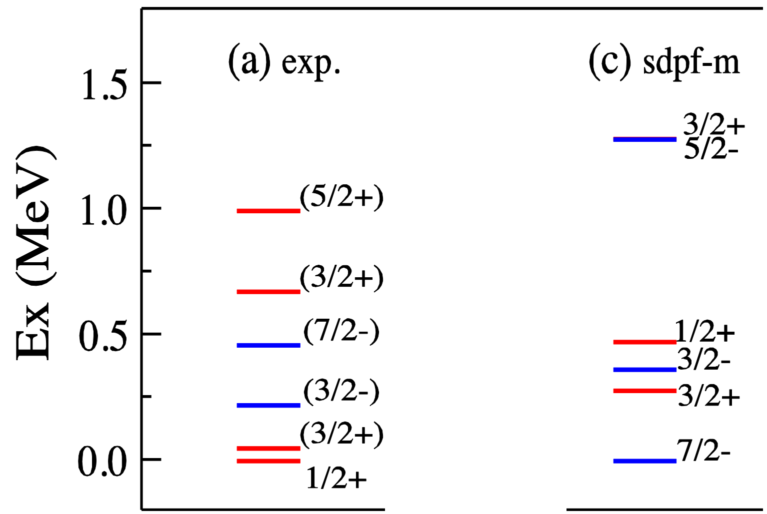

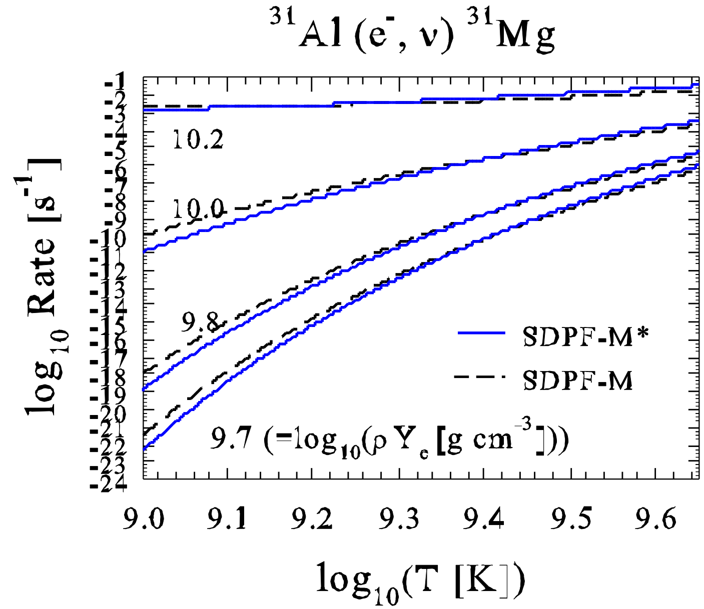

SDPF-M

SDPF-M*: E_x & B(GT) = exp.

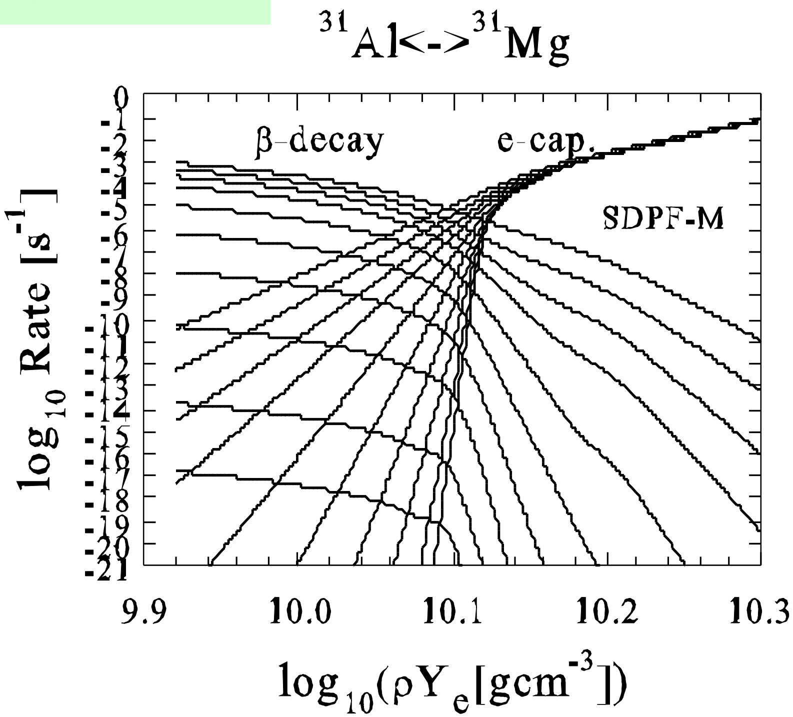

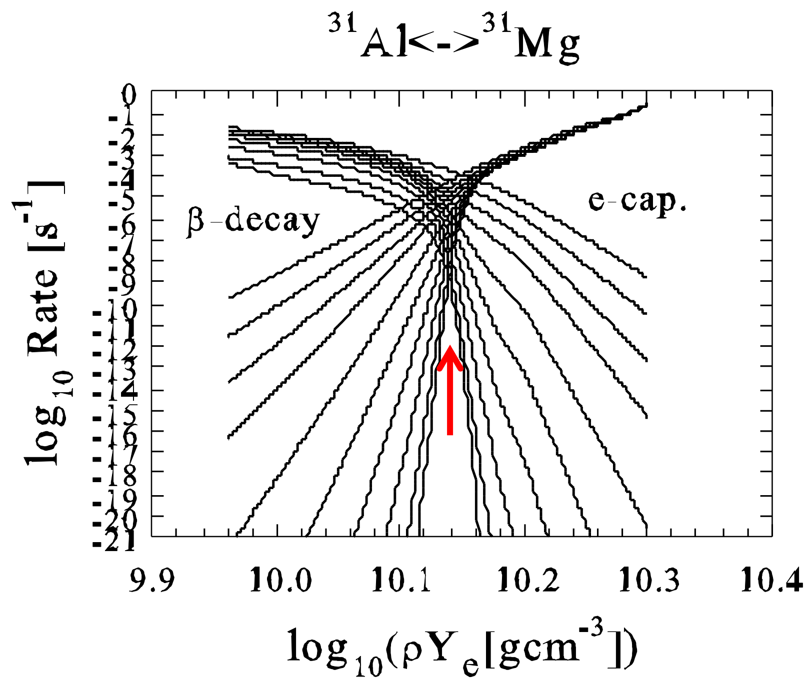

sd-pf shell

Non-degenerate treatment of sd and pf shells by
EKK (extended Kuo-Krenciglowa) method

Tsunoda, Takayanagi, Hjorth-Jensen and Otsuka, Phys. Rev. C 89, 024313 (2014)

Cf: monopoles with non-degenerate vs degenerate method

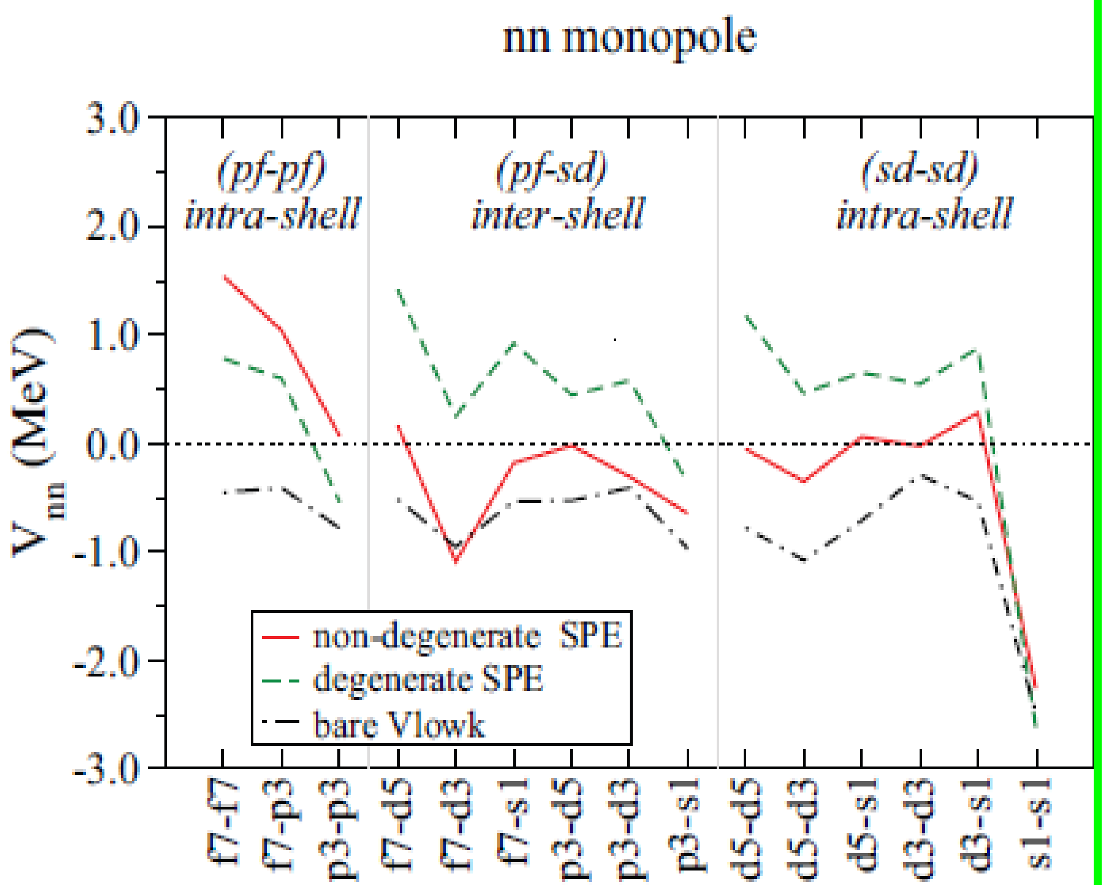

Kuo-Krenciglowa method

$$V_{\rm eff}^{(n)} = \hat{Q}(\epsilon_0) + \sum_{k=1}^{\infty} \hat{Q}_k(\epsilon_0)\{V_{\rm eff}^{(n-1)}\}^k,$$

$$PH_0P = \epsilon_0 P.$$

$$\hat{Q}(E) = PVP + PVQ\frac{1}{E-QHQ}QVP,$$

$$\hat{Q}_k(E) = \frac{1}{k!}\frac{{\rm d}^k\hat{Q}(E)}{{\rm d}E^k}.$$

Extended Kuo-Krenciglowa method

$$\tilde{H} = H - E$$

$$\tilde{H}_{\rm eff}^{(n)} = \tilde{H}_{\rm BH}(E) + \sum_{k=1}^{\infty} \hat{Q}_k(E)\{\tilde{H}_{\rm eff}^{(n-1)}\}^k,$$

$$\tilde{H}_{\rm eff} = H_{\rm eff} - E, \quad \tilde{H}_{\rm BH}(E) = H_{\rm BH}(E) - E,$$

$$H_{\rm BH}(E) = PHP - PVQ\frac{1}{E-QHQ}QVP.$$

$$V_{\rm eff} = H_{\rm eff} - PH_0P.$$

energy indpendent

K. Takayanagi, Nucl. Phys. A 852, 61 (2011).
K. Takayanagi, Nucl. Phys. A 864, 91 (2011).

Neutron-rich isotopes in the island of inversion by EKK-method starting from chiral EFT interaction N^3LO+3N (FM)

Tsunoda, Otsuka, Shimizu, Hjorth-Jensen, Takayanagi and Suzuki, PRC 95, 021304(R) (2017)

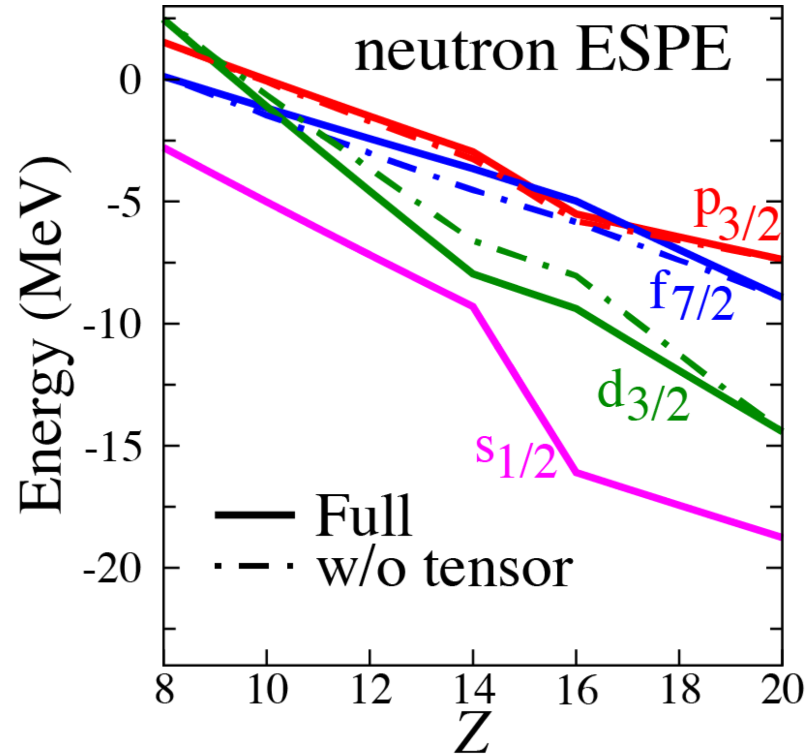

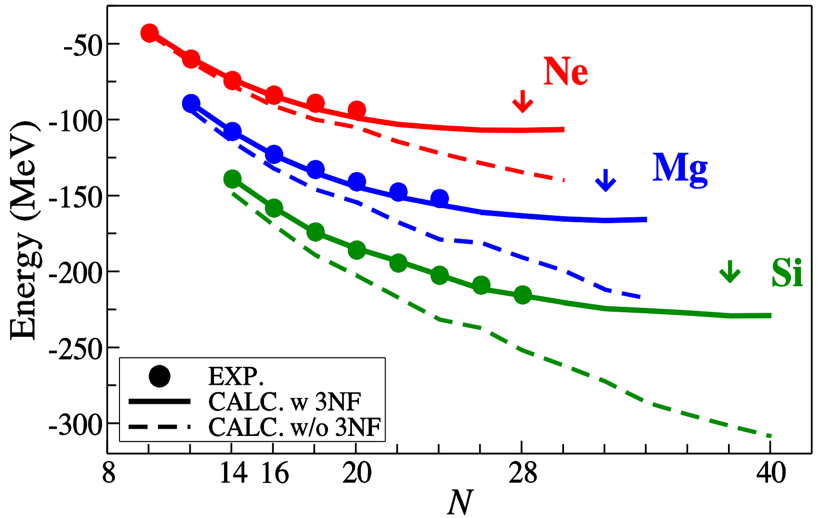

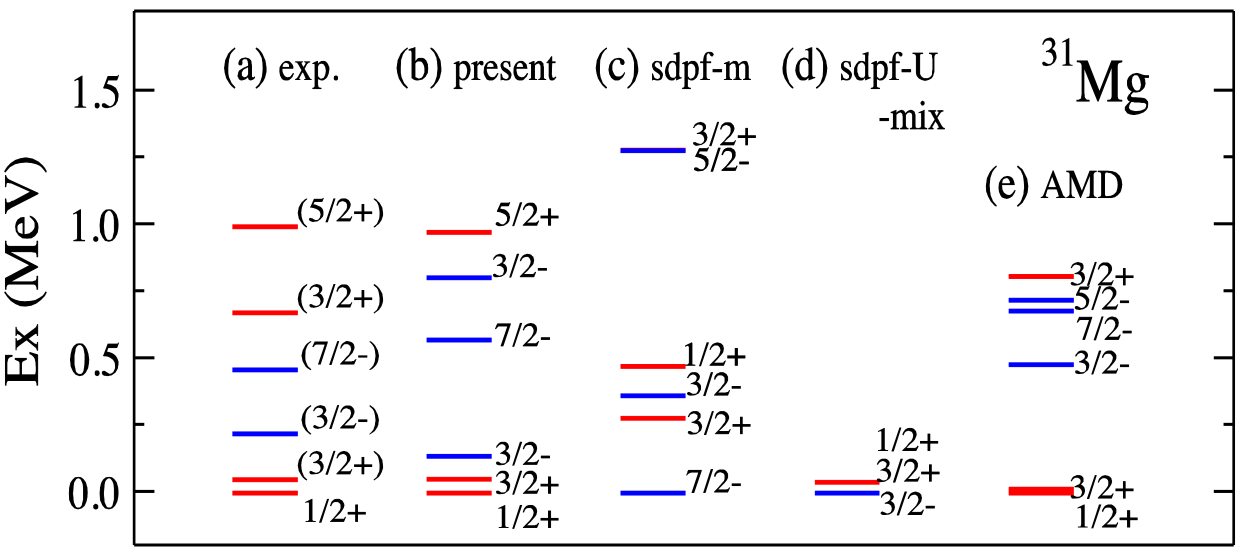

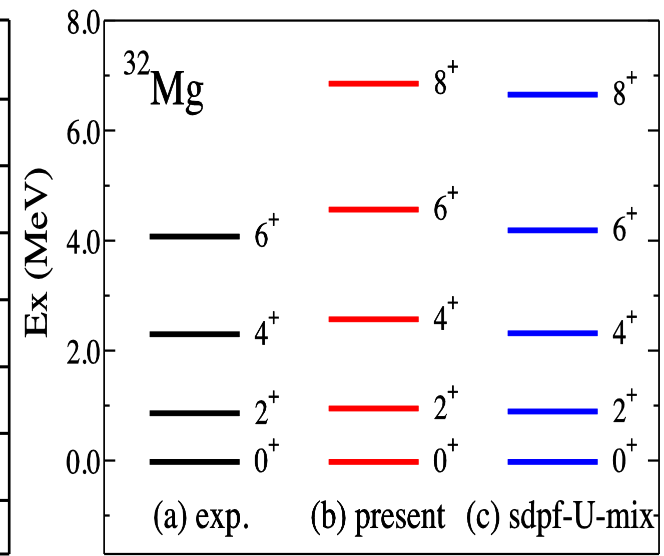

EKK vs EXP

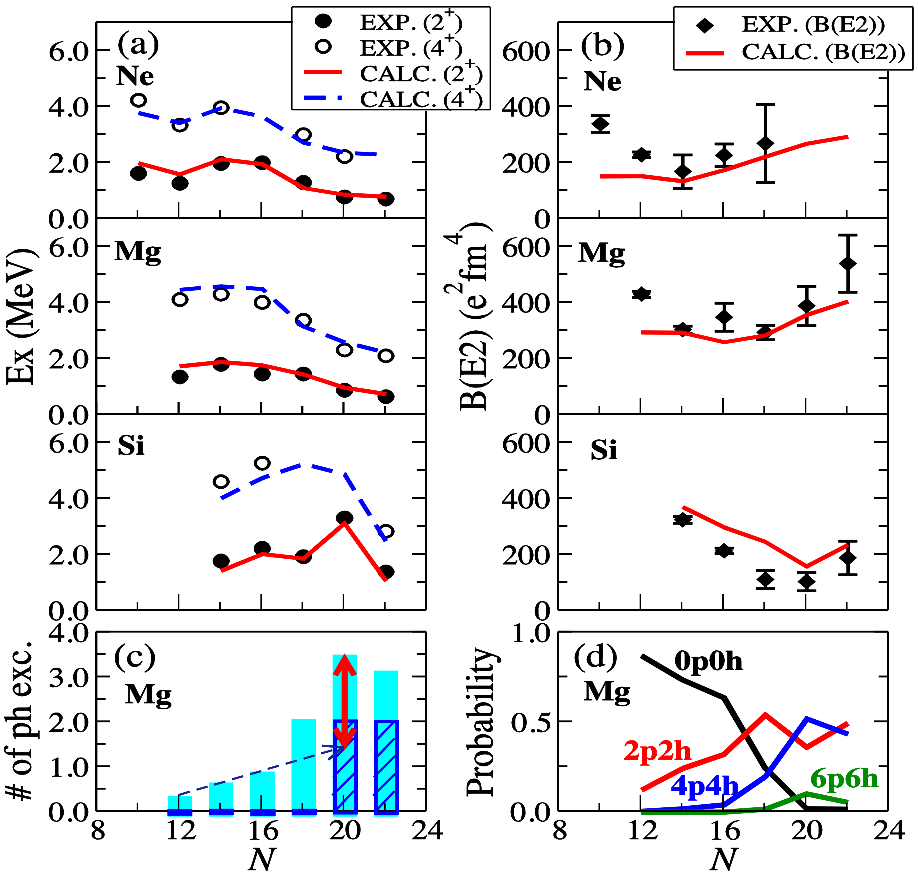

2p-2h+4p-4h

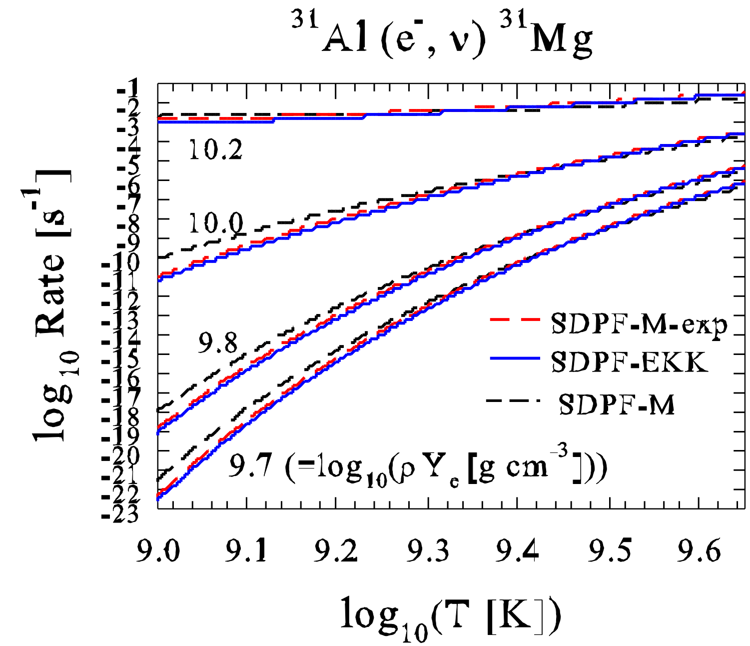

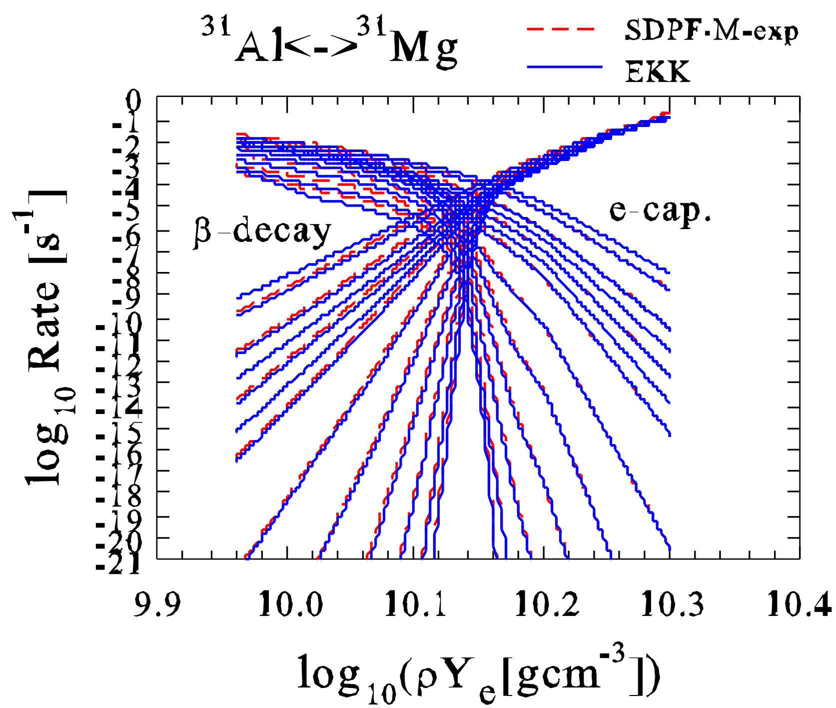

Summary

ν- nucleus reactions

- **New ν –induced cross sections based on new shell-model Hamiltonians with proper tensor forces**
  ^{12}C, ^{13}C, ^{16}O, ^{40}Ar, ^{56}Fe, ^{56}Ni
- **Detection of low-energy reactor, solar ν [^{13}C] and SNν [^{12}C, ^{16}O, ^{40}Ar, ^{56}Fe]**

- **Nucleosynthesis elements by ν-processes**
  ν-^{12}C, ν-^{4}He → ^{7}Li, ^{11}B in CCSNe
  ν-^{56}Ni → ^{55}Mn in Pop. III stars

- **Effects of ν-oscillations (MSW) in nucleosynthesis abundance ratio of $^{7}Li/^{11}B$ → ν mass hierarchy**

- **Cross sections are enhanced by oscillations. Distinguishing mass hierarchy by measurement on earth is not easy because of small E_{split} when both collective and MSW oscillations occur.**

Summary

1. e-capture and β-decay rates for one-major shell nuclei

- **New weak rates for sd-shell from USDB**
  Nuclear URCA processes for A=23 and 25 nuclear pairs
  → Cooling of O-Ne-Mg core of 8-10 solar-mass stars and determines fate of stars with ～9$M_\odot$ whether they end up with e-capture SNe or core-collapse SNe.
- **ab initio interactions vs USDB**
- **New weak rates for pf-shell from GXPF1J**
  Nucleosynthesis of iron-group elements in Type Ia SNe.
  Over-production problem in iron-group nuclei with FFN can be solved with smaller rates with GXPF1J

2. Weak rates for two-major shell nuclei

- **sd-pf shell nuclei in the island of inversion, important for URCA processes in neutron star crusts, are evaluated with EKK method starting from chiral EFT interaction N3LO +3N (FM).**
  e.g. ^{31}Al (e$^-$, ν)^{31}Mg, ^{31}Mg(,e$^-$ ν)^{31}Al

Collaborators

T. Otsuka[m], T. Kajino [b,c], S. Chiba[d],
M. Honma[e], T. Yoshida[c], K. Nomoto[f], H. Toki[g], S. Jones[h],
R. Hirschi[i], K. Mori[b,c], M. Famiano[j], J. Hidaka[k], K. Iwamoto[l],
N. Tsunoda[n], N. Shimizu[n], B. Balantekin[a],

[a]RIKEN
[b]National Astronomical Observatory of Japan
[c]Department of Astronomy, University of Tokyo
[d]Tokyo Institute of Technology
[e]University of Aizu
[f]WPI, the University of Tokyo
[g]RCNP, Osaka University
[h]LANL, [i]Keele University
[j]Western Michigan University, [k]Meisei University
[l]Department of Physics, Nihon University
[n]CNS, University of Tokyo
[m]Univ. of Wisconsin

Note added:

Difference between GXPF1J and KB3G

1. Shell gap $f_{5/2}$-$f_{7/2}$ is larger for GXPF1J
2. Isoscalar pairing is larger for GXPF1J

→ More spreading of GT strength for GXPF1J

Murchison Meteorite

SiC X-grains

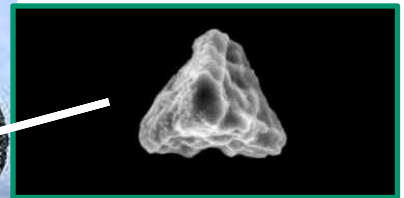

- $^{12}C/^{13}C$ > Solar
- $^{14}N/^{15}N$ < Solar
- Enhanced ^{28}Si
- Decay of ^{26}Al ($t_{1/2}=7\times10^5$yr), ^{44}Ti ($t_{1/2}$=60yr)

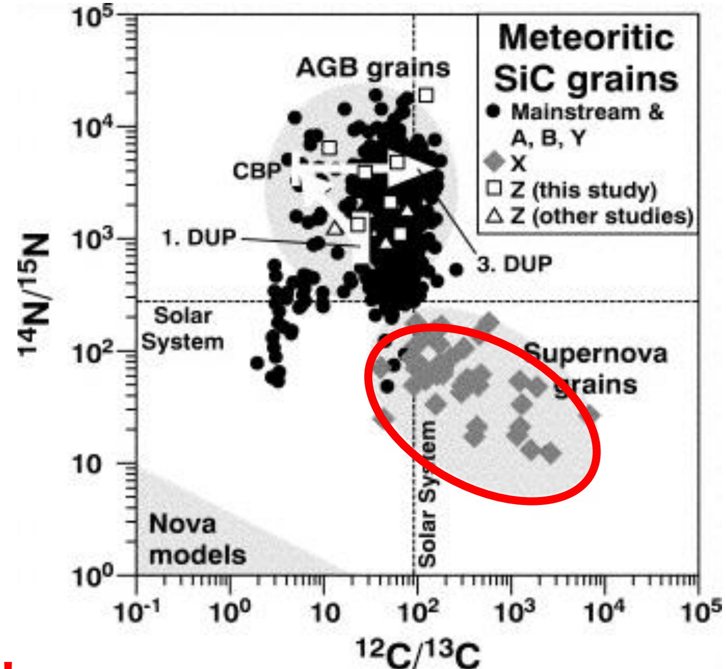

SiC X-grains are made of Supernova Dust !

W. Fujiya, P. Hoppe, and U. Ott (2011, ApJ 730, L7) discovered ^{11}B and ^{7}Li isotopes in 13 SiC X-grains.

Table 1
C-, Si-, Li-, and B-isotopic Compositions of SiC X Grains from the Murchison Meteorite

Grain	Size (μm)	$^{12}C/^{13}C$	$\delta^{29}Si^a$ (‰)	$\delta^{30}Si^a$ (‰)	$^7Li/^6Li$	$^{11}B/^{10}B$	Li/Si (10^{-5})	B/Si (10^{-5})
Single X grains								
X1	0.6	114 ± 2	−178 ± 11	−265 ± 9	11.87 ± 0.63	4.51 ± 0.77	9.69	3.33
X2	1.2	128 ± 2	−377 ± 11	−261 ± 10	12.06 ± 0.62	5.06 ± 0.58	23.8	18.8
X3	1.5	244 ± 5	−205 ± 10	−297 ± 7	11.48 ± 0.86	4.54 ± 0.63	1.76	1.92
X4	1.0	241 ± 6	−556 ± 10	−245 ± 9	12.00 ± 0.56	4.85 ± 1.19	24.8	3.31
X9	0.6	38 ± 1	−361 ± 10	−394 ± 8	11.20 ± 1.01	4.19 ± 0.70	10.8	11.4
X11	0.8	326 ± 14	−358 ± 12	−432 ± 11	11.78 ± 2.03	4.99 ± 1.88	3.66	3.00
X13	0.7	345 ± 6	−261 ± 10	−424 ± 7	11.59 ± 0.93	4.37 ± 2.04	10.7	1.14
Average					11.83 ± 0.29	4.68 ± 0.31		
X grains + other nearby/attached SiC grains								
X5		34 ± 1	−226 ± 11	−120 ± 10	12.21 ± 0.41	4.36 ± 0.40	40.2	18.8
X6		88 ± 1	−236 ± 11	−189 ± 9	13.06 ± 1.36	3.83 ± 0.27	2.15	14.2
X7		78 ± 1	−281 ± 11	−208 ± 10	11.20 ± 2.40	11.47 ± 6.36	8.28	9.48
X8		76 ± 1	−223 ± 10	−266 ± 8	11.29 ± 0.64	4.27 ± 0.29	4.80	12.4
X12		83 ± 1	−271 ± 11	−242 ± 10	11.54 ± 0.52	4.13 ± 0.46	24.3	14.2
Average					11.90 ± 0.28	4.16 ± 0.17		
Solar		89	0	0	12.06	4.03	5.6	1.9

Note. $^a\delta^iSi = [(^iSi/^{28}Si)/(^iSi/^{28}Si)_\odot - 1] \times 1000$.

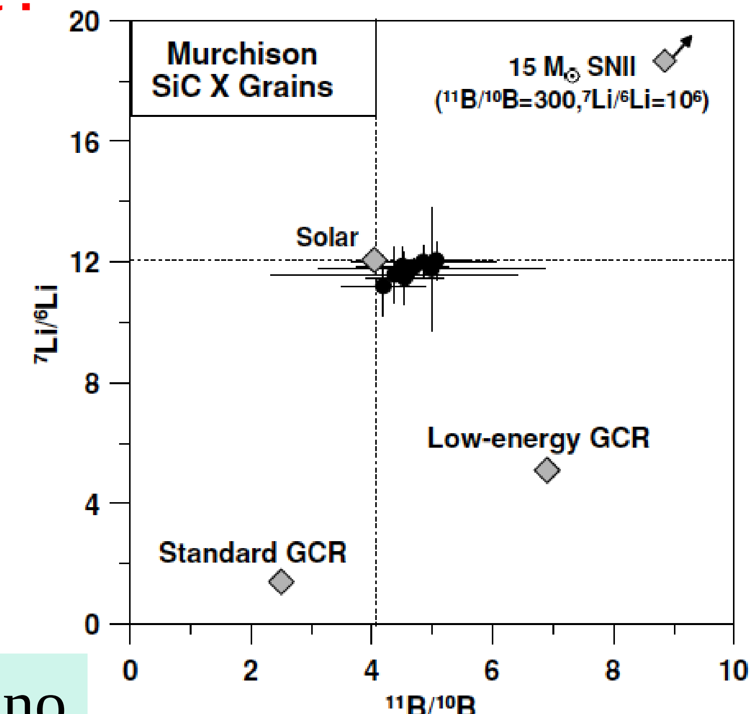

Kajino